DOT/FAA/AR-TT09/42

Air Traffic Organization
NextGen &Operations Planning
Office of Research and
Technology Development
Washington, D.C. 20591

Vaporization of JP-8 Jet Fuel in a Simulated Aircraft Fuel Tank Under Varying Ambient Conditions

August 2009

Technical Thesis

The research described in this report was funded by the FAA as part of its mission to improve aircraft safety. The views and opinions expressed are those of the author alone and do not necessarily represent the views of the FAA. The FAA assumes no liability for the contents or use thereof. The FAA has not edited or modified the contents of the report in any manner.

This document is available to the U.S. public through the National Technical Information Service (NTIS), Springfield, Virginia 22161.

U.S. Department of Transportation
Federal Aviation Administration

NOTICE

This document is disseminated under the sponsorship of the U.S. Department of Transportation in the interest of information exchange. The United States Government assumes no liability for the contents or use thereof. The United States Government does not endorse products or manufacturers. Trade or manufacturer's names appear herein solely because they are considered essential to the objective of this report. This document does not constitute FAA certification policy. Consult your local FAA aircraft certification office as to its use.

This document represents the views of the author and does not represent the views of the FAA. The FAA assumes no liability for the contents or use thereof. The FAA has not edited or modified the contents of the report in any manner.

Technical Report Documentation Page

1. Report No.	2. Government Accession No.	3. Recipient's Catalog No.
DOT/FAA/AR-TT09/42		

4. Title and Subtitle	5. Report Date
VAPORIZATION OF JP-8 JET FUEL IN A SIMULATED AIRCRAFT FUEL TANK UNDER VARYING AMBIENT CONDITIONS	August 2009
	6. Performing Organization Code
7. Author(s)	8. Performing Organization Report No.
Robert Ian Ochs	
9. Performing Organization Name and Address	10. Work Unit No. (TRAIS)
Federal Aviation Administration William J. Hughes Technical Center Airport and Aircraft Safety Research and Development Division Fire Safety Team Atlantic City International Airport, NJ, 08405	11. Contract or Grant No.
12. Sponsoring Agency Name and Address	13. Type of Report and Period Covered
U.S. Department of Transportation Federal Aviation Administration NextGen & Operations Planning Office of Research and Technology Development Washington, DC 20591	Technical Thesis
	14. Sponsoring Agency Code ANM-112

15. Supplementary Notes

The Federal Aviation Administration Airport and Aircraft Safety R&D Division Technical Monitor was Fred Snyder. This work was conducted in partial fulfillment of the degree requirements for a Master's degree in Mechanical and Aerospace Engineering, which was awarded to the author by Rutgers, The State University of New Jersey, New Brunswick, New Jersey in May 2005.

16. Abstract

This study has been performed to aid in the effort to minimize the possibility of a fuel tank explosion in a commercial aircraft. An understanding of the mechanisms behind fuel vaporization processes in an aircraft fuel tank is essential to developing accident prevention techniques. An experiment was designed to measure the conditions existing within a heated aluminum fuel tank, partially filled with JP-8 jet fuel, under varying ambient conditions similar to those encountered by an in-flight aircraft. Comprehensive fuel tank data, including all temperatures, pressure, and ullage hydrocarbon concentration, was obtained during testing, and is available for use to validate heat and mass transfer calculations. An existing model was employed in this work to calculate ullage temperature and ullage fuel vapor concentration in the tank and compare with measured values, to explain the transport processes occurring in the tank during testing, and to estimate the flammability of the ullage vapors existing within the tank. The calculations made by the model were in good agreement with the measured data. The model also gave a good indication of the temporal mass transport processes occurring in the tank and gave a reasonable assessment of the ullage vapor flammability in the tank.

17. Key Words	18. Distribution Statement
JP-8, Jet fuel, Vaporization, Fuel tank, Flammability, Modeling	This document is available to the U.S. public through the National Technical Information Service (NTIS) Springfield, Virginia 22161.

19. Security Classif. (of this report)	20. Security Classif. (of this page)	21. No. of Pages	22. Price
Unclassified	Unclassified	86	

VAPORIZATION OF JP-8 JET FUEL IN A SIMULATED AIRCRAFT FUEL TANK UNDER VARYING AMBIENT CONDITIONS

BY ROBERT IAN OCHS

A Thesis submitted to the

Graduate School-New Brunswick

Rutgers, The State University of New Jersey

In partial fulfillment of the requirements

for the degree of

Master of Science

Graduate Program in Mechanical & Aerospace Engineering

written under the direction of

Professor C.E. Polymeropoulos

and approved by

_____

_____

_____

New Brunswick, New Jersey

May 2005

ABSTRACT OF THE THESIS

VAPORIZATION OF JP-8 JET FUEL IN A SIMULATED AIRCRAFT FUEL TANK UNDER VARYING AMBIENT CONDITIONS

BY ROBERT IAN OCHS

Thesis Director:
Professor C.E. Polymeropoulos

This study has been performed to aid in the effort to minimize the possibility of a fuel tank explosion in a commercial aircraft. An understanding of the mechanisms behind fuel vaporization processes in an aircraft fuel tank is essential to developing accident prevention techniques. An experiment was designed to measure the conditions existing within a heated aluminum fuel tank, partially filled with JP-8 jet fuel, under varying ambient conditions similar to those encountered by an in-flight aircraft. Comprehensive fuel tank data, including all temperatures, pressure, and ullage hydrocarbon concentration, was obtained during testing, and is available for use to validate heat and mass transfer calculations. An existing model was employed in this work to calculate ullage temperature and ullage fuel vapor concentration in the tank and compare with measured values, to explain the transport processes occurring in the tank during testing, and to estimate the flammability of the ullage vapors existing within the tank. The calculations made by the model were in good agreement with the measured data. The model also gave a good indication of the temporal mass transport processes occurring in the tank and gave a reasonable assessment of the ullage vapor flammability in the tank.

ACKNOWLEDGEMENTS

First and foremost I would like to thank Professor Constantine Polymeropoulos for his professional and personal guidance and many, many useful and enlightening discussions on the topics of aviation fuel properties, heat and mass transfer, modeling fuel vaporization, and experimental methods and procedures. His leadership and direction has been most valuable during my time spent here at the university.

I would also like to thank Mr. Richard G. Hill and Mr. Gus Sarkos at the Fire Safety Branch of the Federal Aviation Administration's William J. Hughes Technical Center for the opportunity to perform this research at the technical center and for the many conversations with them about fuel tank safety. Their knowledge, wisdom, and insight on the subject of fuel tank safety is truly unmatched, and was extremely valuable in writing this thesis.

I would like to thank Mr. Steven Summer and Mr. Joseph DeFalco for their help in the development of the experimental apparatus, assistance in obtaining materials required to complete the research, and many useful discussions about fuel tank safety. Much thanks and appreciation also goes to the entire staff of the Fire Safety Branch of the Federal Aviation Administration's William J. Hughes Technical Center for aiding in completing this research.

I would also like to thank the Department of Mechanical and Aerospace Engineering for the ability to study under the tutelage of the many professors with diverse academic backgrounds and great knowledge of the engineering sciences.

DEDICATION

This thesis is dedicated to my parents, Richard C. Ochs and Florence J. Ochs. Their endless love and tireless efforts have been of great help during these times and truly reflect in my achievements in academia and accomplishments in life.

TABLE OF CONTENTS

LIST OF FIGURES

LIST OF TABLES

1.0 INTRODUCTION

1.1 Background

Since the achievement of flight just over one hundred years ago, the skies have become the means by which millions of travelers get to their destinations quickly, comfortably, and economically. Statistically, air travel is quite safe, when comparing the number of accidents with the number of hours in flight. Although aircraft accidents are tragic events, much can be learned from piecing together the events leading to an accident. Accident investigations, combined with modern technological analyses, have paved the way for safer flying due to a better understanding of the cause of accidents. Aviation authorities use the results from accident investigations to impose regulations upon airlines and aircraft manufacturers to prevent future accidents and loss of life.

The focus of this work is the study of fuel tank flammability, an area that has gained much attention since the catastrophic mid-air breakup of TWA flight 800 after takeoff from J.F.K. airport on Long Island, New York in July 1996. Flight 800, a Boeing 747-131, suffered a crippling fuel tank explosion that resulted in the structural failure of the aircraft and, unfortunately, the loss of life of every person on board [1]. Accident investigators from the National Transportation Safety Board (NTSB) have determined the cause of the crash was an explosion in a nearly empty center wing tank (CWT) caused by an unconfirmed ignition source [2]. An explosive condition in the CWT resulted because combustible vapor was generated from heating of the fuel in the tank.

The potential flammability of fuel tanks has been recognized for some time now, and research has been performed by the military and government starting in the 1950's through present day to study the flammable characteristics of jet fuel [3, 4] and to

develop procedures to lessen the likelihood of an accident [5]. Early studies were performed to determine the flammability limits of jet turbine fuel within aircraft fuel tanks [3, 4, 6], the effect of ullage space on the lower flammability limit [2], and the effect of cold ambient temperatures on flammability [7], among other topics. More recently the direction of research has turned towards inerting fuel tanks with an inert gas (nitrogen) in order to lower the oxygen concentration below the lowest oxygen concentration (LOC) that will support ignition of fuel vapor [8, 9]. The LOC is a critical number for designing an inerting system; therefore extensive research was focused on finding the LOC at different ambient pressures and ignition energies, as well as with several different ignition sources [9]. The fuel vapor composition has been found to be quite critical to the overall flammability and ignitability of vapor-air mixture in a fuel tank [10]. Understanding the vaporization and condensation processes of liquid fuel and applying it to modeling a dynamic fuel tank system [11] can provide much insight into the periods during which a fuel tank may be considered dangerously flammable. Much of this research was performed with the overall goal of reducing and hopefully eliminating the possibility of ever having a fuel tank explosion in commercial airliners.

1.2 Flammability in Fuel Tanks

Figure 1.1 shows a diagram of a Boeing 747 and the locations of the fuel tanks. The fuel on commercial airliners is first loaded in fuel tanks in the wing structures. These fuel tanks are in direct contact with the outside skin of the wing, and therefore are exposed to the outside air, which is very cold (-70°F) at cruising altitudes (40,000 ft.) [13]. This reduces the possibility of having a flammable mixture in the wing fuel tanks in flight,

since jet fuel is typically not flammable under 100°F [13]. On the ground, the top wing surfaces can be heated by sunlight. However, this is generally not a critical condition because the liquid fuel is on the bottom fuel tank surface, and significant time is required to heat the liquid to create a flammable mixture. The extra fuel required for larger aircraft, such as a Boeing 747, is carried in the center wing tank, which is located in the structural wing box within the fuselage and beneath the cabin. Figure 1.2 shows a schematic of a Boeing 747 center wing tank. On flights where the fuel in the wing tanks is sufficient to reach the destination, the CWT is left empty to save weight and increase fuel efficiency [13].

In the case of TWA 800, the CWT had a fuel capacity of 12,890 gallons, but contained only 50 gallons of fuel [2]. This small amount of fuel in the tank formed a very thin liquid layer across the bottom surface, and any heat input into this fuel layer could rapidly raise its temperature to above the flash point of the fuel, thus forming combustible vapors in the ullage space. In some large commercial airliners with CWT's, environmental control system air conditioning packs (ECS packs) are located underneath the CWT. These ECS packs "reduce the temperature and pressure of hot bleed air from one or more of the airplane's engines, the APU (auxiliary power unit), or the high-pressure ground power carts during ground operations, to provide environmental control (pressurization, ventilation, and temperature) to the cockpit and the main cabin" [13]. These packs remove heat from the hot bleed air and essentially use the CWT and surrounding areas as a heat sink to dissipate the heat, thus raising the temperature of the liquid fuel in the CWT.

When it was determined that a CWT explosion was the cause of the breakup of flight 800, the NTSB responded by issuing several safety recommendations to the FAA. One of these recommended that (aircraft) “maintain sufficient amounts of fuel in the CWT’s of transport aircraft to limit the liquid fuel temperature rise and evaporation, thus keeping the vapor fuel/air ratio below the explosive limit” [2]. Currently, researchers are looking for better ways to reduce flammability in fuel tanks. On-board inert gas generating systems (OBIGGS) have been developed by the FAA [8] and private industry. These systems use hot engine bleed air to create nitrogen-enriched air (NEA) via hollow fiber membrane air separation modules. The NEA is forced into the CWT until the oxygen concentration is reduced below the lower oxygen concentration (LOC) under which no combustion can be sustained [9].

Modeling of the fuel vaporization and condensation processes in a tank can give insight into situations in which the fuel tank is vulnerable to explosion, and the threshold of vapor flammability can then be estimated. The LOC and the flammability calculations can then be combined to determine the requirements necessary for an inerting system to provide a non-explosive condition in a fuel tank.

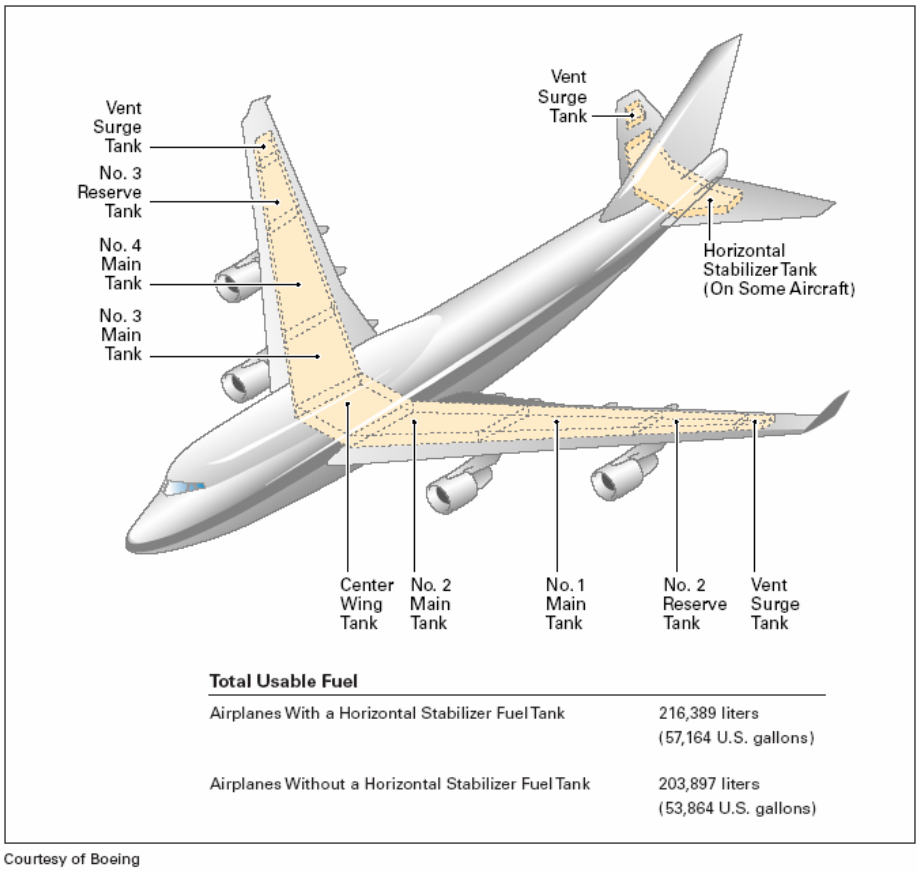

Courtesy of Boeing

Figure 1.1. Diagram of a Boeing 747-400 with locations of all fuel storage tanks.

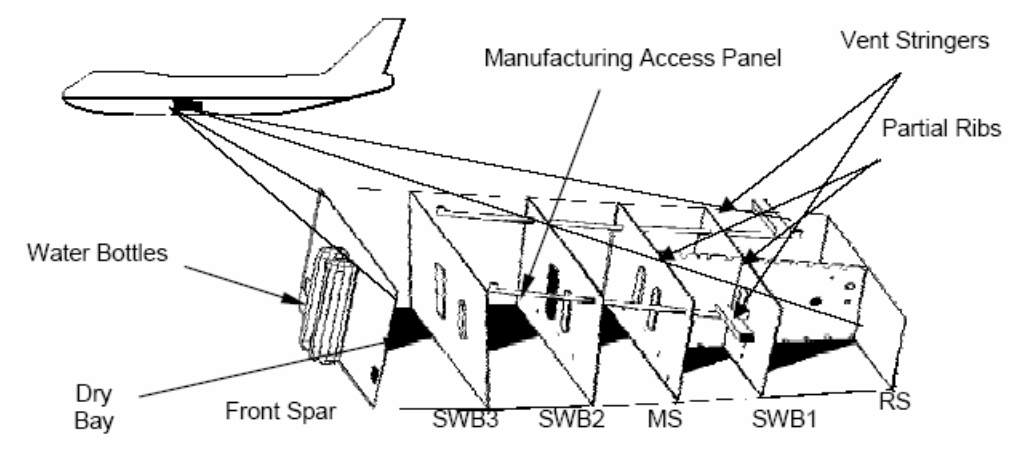

Figure 1.2. Schematic of the 747-100 CWT with locations of the different bays.

1.3 Objectives of the Thesis

The ultimate goal for fuel tank protection research is to determine methods, or procedures, that can eliminate the possibility of fuel tank fires and explosions. Fuel vaporization modeling can be used to estimate the fuel vapor concentration in the ullage of a fuel tank as a function of the tank pressure and temperature. Such a model can be valuable to the fuel tank protection cause, as computer modeling reduces the cost and time of full-scale experimentation. The model calculations can also be used for fuel tank inerting requirements or to verify the intrinsic safety of an inert fuel tank. The objective of this study is to generate experimental data on fuel vaporization for tank conditions appropriate to those encountered in an aircraft fuel tank. The data obtained can then be available for validating the estimations from vaporization models.

To that effect, an experiment was designed to simulate an in-flight environment around a fuel tank and measure tank conditions. The experimental setup consisted of a simulated fuel tank with a uniformly heated floor surface and unheated sidewalls and top surface. The tank was instrumented with thermocouples and a total hydrocarbon detector for measuring the vapor concentration in the ullage gas. The fuel tank was situated in an environmental chamber that could vary the ambient pressure and temperature to simulate flight conditions. Data was collected for different pressure and temperature conditions using JP-8 as the evaporating liquid. A limited number of tests were also performed using isooctane (2-2-4 trimethylpentane) as the test liquid. The data was compared with predictions from an available fuel vaporization model [11] that was also used to assess the flammability of the vapor generated and for discussion of the overall transport processes occurring within the fuel tank.

2.0 REVIEW OF LITERATURE

2.1 Jet Fuels

2.1.1 History of Jet Fuel

Jet fuels have changed significantly over the last sixty years. The first British jet engine, patented by Sir Frank Whittle in 1930 and first flown in 1941, was designed to run on illumination kerosene, as gasoline was in short supply during World War II [14]. The first U.S. jet engines were direct copies of this original design, and adopted kerosene as well for the primary fuel in U.S. jet turbines. The first U.S. jet fuel specification, AN-F-32, was made in 1944 and was designated JP-1, a kerosene with a flashpoint of 109°F and freeze point of -77°F [14]. JP-1 had limited availability, and was soon replaced by wide cut fuels, which are mixtures of hydrocarbons that span the gasoline and kerosene boiling point ranges [14]. The military version of the wide cut fuel, JP-4, was used by the U.S. military from 1951 to 1995, and the commercial equivalent Jet-B was used in airliners. The wide cut fuel had a flash point of about 0°F and freeze point of -77°F. This low flash point indicates that the wide cut fuels were quite volatile, like gasoline, which has a flash point of about -40°F, and that the risk of fire during fuel handling and crash was great, as were evaporative losses at altitude. It was for these reasons that a non-wide cut fuel was sought with a higher flashpoint temperature for safety and a higher freeze point temperature for wider availability.

The specifications for Jet-A and Jet-A1 were made in the 1950's for commercial use, and have a minimum flashpoint specification of 100°F and freeze points of -40°F and –47°F, respectively. The U.S. military equivalent of Jet-A is JP-8, and has been in use since the changeover from wide cut JP-4 in 1995. JP-8 is very similar to Jet-A but

has more additives, such as an antistatic additive and an icing inhibitor [15]. Table 2.1, with information from ref. [14] and [15], shows a comparison of the flash and freeze points of the various fuels from over the years.

Table 2.1. Comparison of Aviation Turbine Fuel Properties

Fuel Type	*Min. Flash Point (°F)*	*Max Freeze Point (°F)*	*Years in Use*
JP1	109	-77	1944-47
JP4	0	-77	1951-95
JP5	140	-51	1952-present
JP6	140	-66	1956(XB-70)
JP7	140	-47	1960's(SR-71)
JP8	100	-53	1978-present
Jet A	100	-40	1950's-present
Jet A-1	100	-47	1950's-present

ASTM D 1655 is the current standard that lists the specifications for three types of jet fuels: kerosene based Jet-A, Jet A-1 and the wide cut Jet-B. There are at least 23 specifications for Jet-A, which set maximum and minimum limits for stated properties or measurements [13]. These specifications, however, do not require an exact composition of chemical species (Jet-A has hundreds of different components); rather, they specify that “aviation turbine fuel shall consist of refined hydrocarbons derived from crude petroleum, natural gasoline, or blends thereof with synthetic hydrocarbons [16].” Since exact composition is not required, Jet-A and the military grade equivalent JP-8 can typically consist of hundreds of compounds. Analysis has shown that Jet-A consists of about “75%-85% paraffin, both straight chain and cyclic, with the balance almost entirely aromatic compounds” [13].

2.1.2 Fuel Flash Point

The flash point is defined as the lowest temperature at which a liquid can form an ignitable mixture in air near the surface of the liquid. It is determined by the ASTM D56 standard, which is commonly referred to as the Tag closed cup test. In this test, a small sample (50 ml) is placed in a closed cup (130 ml), corresponding to a mass loading of 300 kg/m^3, surrounded by a water bath. The sample is gradually heated at 2°F per minute, and a small flame is introduced into the vapor space at regular temperature intervals for one second. The temperature at which the first ignition, or "flash", is observed is the flash point of the fuel. ASTM D 1655 specifies a minimum flash point of 100°F for Jet-A. This is very high when compared to gasoline, which has a flash point of about -40°F. It is important to remember that the fuel flash point "is not a fundamental property but rather the result of a standardized test carried out at one specific fuel loading and atmospheric pressure" [17]. Also, the flash point, while a good reference when comparing the flammability of one fuel to another, cannot give a precise indication of the overall flammability of a mixture for multi-component fuels. This is because the flash point, as determined by standardized testing, is dependent upon the vapor composition, which has been shown to vary for multi-component fuels as a function of temperature and mass loading [17].

2.1.3 Fuel Vapor Pressure

Liquid in a closed container will form vapor in the space above the liquid surface until the space becomes saturated. At this point, known as equilibrium, the rate of molecules leaving the liquid equals the rate of molecules returning to the liquid surface. This

equilibrium is dynamic in nature, because while the concentrations in the vapor and liquid are not changing, the molecules are still moving from liquid to vapor and vice versa; but the rates are equal, giving rise to equilibrium. The vapor pressure is the pressure measured in the vapor space at equilibrium; it is dependent upon temperature only. The temperature dependence arises from the Maxwell-Boltzmann distribution of kinetic energies in a collection of molecules. At a given temperature, only a certain number of molecules have enough kinetic energy to overcome the intermolecular forces holding them in the liquid. Thus, by increasing the temperature of the liquid, the distribution of molecules with enough kinetic energy to escape will broaden, giving rise to more molecules leaving the liquid, effectively increasing the vapor pressure and concentration in the space above the liquid.

In a vented container, such as a fuel tank, at low ambient pressures (high altitudes) there will be less air in the space above the liquid as a result of venting due to pressure equalization between the inside of the tank and the atmosphere. If the liquid in the container remains at a constant temperature during ambient pressure drop, the liquid vapor pressure must remain constant as well. Since less air exists in the ullage at high altitudes, the overall volumetric concentration of fuel in the ullage increases. It is for this reason that at high altitudes the volumetric concentration of fuel molecules in the ullage will be higher than at sea level for a liquid at a constant temperature.

2.1.4 Mass Loading

The fuel mass loading is a convenient way of describing the mass of fuel in a tank relative to the volume of the fuel tank containing it; it is defined as the mass of fuel per

unit volume of the fuel tank. For example, if the tank is full of fuel, the mass loading is equal to the density of the fuel; if the tank is half full, the mass loading is equal to half the density, and so forth. At the time of explosion, the CWT of TWA 800 had a mass loading of approximately 3 kg/m^3. This is a very small amount of fuel in a very large tank, about 0.37% full. For such a minimal mass loading, the liquid forms a very thin layer on the bottom surface of the tank, and if the tank floor is heated, the temperature of the liquid can raise drastically, increasing the rate of fuel vaporization and the amount of fuel in the ullage. Research has been performed to determine the mass loading effects on the fuel vapor concentration in the ullage. It was determined that, in order to significantly decrease the amount of vapor evolving into the ullage, the fuel loading has to be extremely low, between 0.15 and 0.08 kg/m^3 [2].

2.1.5 Multicomponent Fuel Vaporization

Liquids fuels with several components are typically referred to as multicomponent fuels, Jet A and JP-8 being perfect examples. As mentioned earlier, jet fuels have hundreds of different chemical components, each component having unique chemical properties such as molecular weight, boiling point, and vapor pressure. The overall liquid fuel takes on unique properties that depend entirely upon the quantity and properties of the individual components. Equilibrium vapor pressure calculations can be made for a fuel with a known composition that account for the vapor pressures of the individual components. Likewise, the percentage of each component in the liquid fuel can be used to determine the amount of each component vaporizing at a specified liquid temperature. The critical

factor in making these calculations is knowledge of the fuel composition, which varies greatly from batch to batch and is largely unknown.

2.1.6 Characterization of Multicomponent Jet Fuel

Jet-A and JP-8 are very complex fuels, and, as stated earlier, are governed by ASTM specifications for performance and safety, but not for composition. Knowledge of the composition of the liquid fuel is important for predicting the composition and concentration of fuel in the fuel-air mixture in the ullage and assessing the level of flammability in a fuel tank. Jet fuel samples have been characterized by speciation at and near the flashpoint using a gas chromatograph combined with a flame ionization detector. It was determined that over 300 hydrocarbons could be used to completely characterize Jet-A and JP-8 [20]. Although speciation is a comprehensive way to quantify the components in the fuel, it is not the most efficient or effective method.

Woodrow has shown [21] that for prediction of the overall vapor pressure of JP-8 samples at temperatures appropriate to those of a fuel tank, it is sufficient to characterize the fuel using a number of *n*-alkane reference hydrocarbons as determined by gas chromatography. This approach effectively reduced the number of components from over 300 to sixteen (C5 to C20 alkanes). Woodrow's work [21] thus presents the liquid compositions of JP-8 samples with different flash points, in terms of the mole fractions of C5-C20 normal alkanes. Since fuels of varying compositions could be represented by their respective flashpoints, it is evident that the fuel flashpoint, and hence the flammability, is dependent upon the composition of the fuel.

It was shown that the fuel vapor composition as well as the vapor to liquid volume ratio (V/L) had significant effects on the vapor pressure and the flashpoint [21]. The vapor pressure decreased with increasing sample flashpoint, due to the abundance of lighter low molecular weight-high vapor pressure hydrocarbons in the low flash point samples, while the fuel samples with higher flash points had higher concentrations of heavy, high molecular weight-low vapor pressure hydrocarbons. For samples with the same flash point, decreasing the V/L ratio decreased the vapor pressure, due to the depletion of high vapor pressure hydrocarbons at the low V/L ratio. The significance of these findings is that the variation of flash point among samples of Jet-A reflects the relative concentration between high and low vapor pressure components which control the low temperature vaporization processes typically seen in a fuel tank.

The fuel used in this experimentation was tested for flashpoint in order to determine which of the characterized fuels [21] would be best suited for modeling the experiments. The experimental fuel had a measured flashpoint of 117°F, therefore, the two fuel compositions from ref. 21 chosen to “bracket” the fuel composition used in the present experiments were the fuels with flashpoints of 115°F and 120°F. Figure 2.1 shows the distribution of *n*-alkane species by number of carbon atoms in the two fuel compositions chosen from ref. 21. It is apparent that the 115 °F flashpoint fuel has a higher concentration of low molecular weight-low boiling point species than the 120°F flashpoint fuel, which has a broader range over the high molecular weight-high boiling point species. This figure helps to visualize the fact that fuels with higher concentrations of light components will have lower flashpoints and be more flammable than fuels with higher concentrations of heavy components.

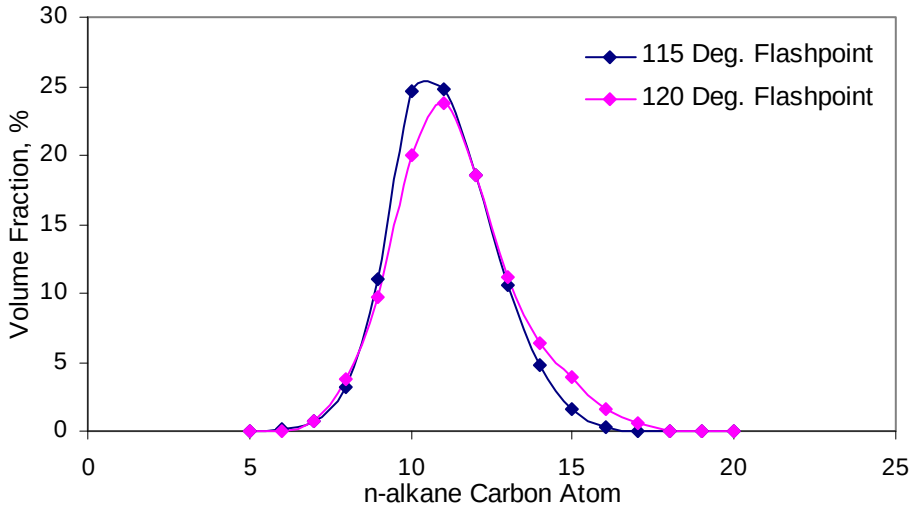

Figure 2.1. Distribution of *n*-alkane components by carbon atoms in two fuels with flashpoints of 115°F and 120°F, from [21].

2.1.7 Flammability Limits

The flammability limits of a fuel-air mixture are defined as "the leanest and richest concentrations that will just self-support a flame [22]." These two points define a flammability range at a specified pressure. As the temperature and pressure are both decreased, these two points typically converge, and likewise as the temperature and pressure are increased the two points diverge, making a flammability envelope, outside of which no flammable mixtures exist, as shown qualitatively in figure 2.2. Addition of inert diluents, such as CO_2, N_2, Ar, He, or halogen compounds, into the vapor space have the effect of converging the flammability limits or even eliminating flammability altogether [22]. This is the basis in developing nitrogen inerting systems for commercial and military aircraft fuel tanks [8].

Intuition would lead to the belief that at the lower flammability limit the fuel is at the flashpoint temperature, since the flashpoint is the lowest fuel temperature that will

support ignition and the lower flammability limit is the leanest mixture that will support ignition. However, the flashpoints are generally higher than dictated by the lower flammability limit temperature due to nonequilibrium conditions in the testing, different modes of ignition, and the inherent nonconservatism in representing real upward flame propagation by a device with downward propagation [13]. It was also found that, in general, the FAR at the flashpoint was at least 15% greater than at the lower limit, although the data had much scatter [13]. For multicomponent fuels, since the vapor composition varies from that of the liquid, relative liquid-vapor mass loading and other factor affect flammability in generally unpredictable ways [13].

The lower flammability limit is the limit of most concern to fuel tank safety researchers. For multicomponent fuels, if the vapor composition is known the lower flammability limit can be estimated using Le Chatelier's rule. Le Chatelier's flammability rule [27] is an empirical formula that correlates flammability limits of multi-component hydrocarbon fuels with the flammability limits of the individual components. It accounts for both the concentration and composition of the fuel-air mixture, and can be calculated by:

$$LC = (1.02 - 0.000721 * T) \sum_{I} \frac{x_i}{LFL_i}, i = 1 \rightarrow N \qquad (2.1)$$

where LC is the calculated Le Chatelier ratio, the first term in parenthesis accounts for temperature compensation, x_i is the i^{th} species mole fraction in the mixture, LFL_i is the lower flammability limit of the i^{th} species and N is the total number of components in the fuel. The mixture is considered flammable if LC is greater than one.

An empirical criterion used for estimating the fuel to air mass ratio (FAR) at the LFL for most saturated hydrocarbons states that at the LFL the FAR on a dry air basis is

0.035±0.004 at 0°C [26]. The published LFL of JP-8 [37] reflects this approach. Researchers from several institutions involved in the NTSB investigation of the TWA 800 accident [17] used these two methods to calculate fuel flashpoints from experimental fuel analysis data and compared the calculated and measured flashpoints. Both methods yield results that are in reasonable agreement for equilibrium mixtures and can be used for estimating if a given mixture of fuel and air is in the flammable region [17]. It should be noted, however, that there is lack of comprehensive experimental data on the flammability of aviation fuels as a function of temperature and ambient pressure

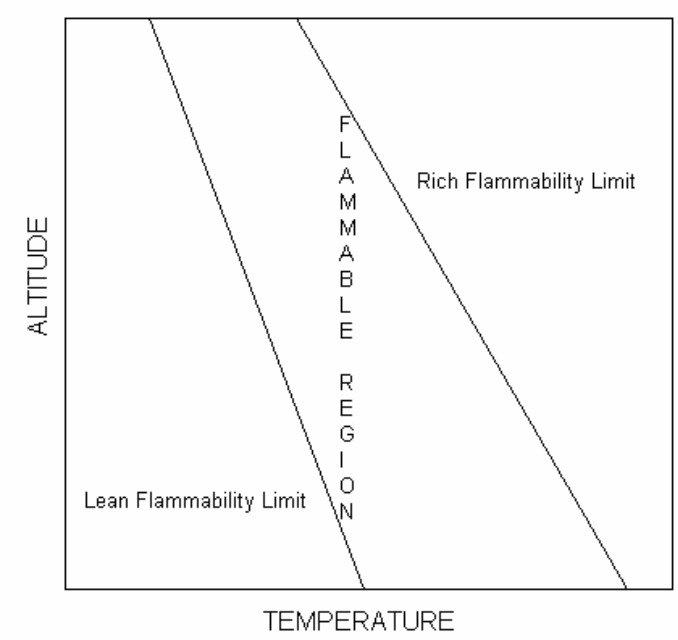

Figure 2.2. Qualitative relation between flammability limits and temperature and altitude (pressure).

2.2 Modeling Fuel Vaporization in a Fuel Tank

Numerous investigators have considered natural convection in enclosures, and examples of reviews on the subject are in refs [30-32]. However, there are few available studies treating the problem of simultaneous heat and mass transfer in enclosures. Reference [23] used detailed numerical modeling of single component vaporization, and computed the formation of flammable vapors in a vented cylindrical vessel. Fuel evaporation within a vented fuel tank was considered in ref [6] using a film model for the vaporization process and an equivalent single component fuel. A similar approach was used in ref [29] for estimation of the fuel to air mass ratio in the tank. Stable and unstable conditions in a tank ullage, the latter leading to free convective mixing, were discussed in ref [33] using a test fuel tank with different wall and liquid heating combinations. Equilibrium air to fuel ratios in a tank were estimated in ref [24] using the Peng-Robinson equation of state and equivalent single and binary component fluids. Heating and vaporization of liquid propane in a tank exposed to a fire, and the resulting explosion hazard from the pressure buildup were discussed in ref [34], which includes several citations on the subject.

The present model [11] employed the flow field that developed as a consequence of natural convection between the heated tank floor and the unheated ceiling and sidewalls. It included liquid vaporization of liquid on the test tank floor and condensation on the tank walls and ceiling. For the relatively long test times in ref [2], material and thermal transport within the test tank were considered quasi-steady, and the fluids were assumed to be well mixed based on the magnitude of the gas and liquid phase

Raleigh numbers which were of order 10^9 and 10^5, respectively. This allowed treating the complex natural convection heat and mass transfer processes within the tank using a simplified approach based on empirical heat transfer correlations for the prediction of the temporal variation of the assumed spatially uniform fuel vapor composition within the test tank. The analogy between heat and mass transfer was used for estimating mass transfer coefficients for the multicomponent evaporation and condensation processes considered. Available experimental data on tank wall and liquid fuel temperatures, in combination with overall mass and energy balances, allowed estimation of the composition of the fuel vapor and the gas temperature within the test tank. The model is described in detail in ref [11] and briefly summarized here in the appendix.

2.3 Experimental Research in Fuel Vaporization

Before designing an experiment it was important to consider what experimental setups had been used previously to measure the conditions in an experimental fuel tank. The data required for the computer model is liquid, surface, ullage, and ambient temperatures, ambient pressure, and ullage vapor concentration. The experimental setups in references 2 and 7 were found to be the most useful for the work at hand. In both experiments, an 88.21-ft^3 rectangular aluminum fuel tank was instrumented with 14 K-type thermocouples and a flame ionization detector total hydrocarbon analyzer. Six thermocouples were used to measure ullage temperatures at different heights in the tank and one was used to measure the fuel temperature. Two sample ports, which could be selected by a ball valve, were used to measure vapor concentration at different locations, although it was proven in preliminary experiments that there was no stratification of the

vapor in the ullage. The total hydrocarbon analyzer was calibrated with 4% propane in a nitrogen balance and gave readings in parts per million (ppm) propane from 0 to 10^4. The output of the analyzer was then converted to fuel to air mass ratio by the relation between FAR, parts per million propane, carbon to hydrogen ratio, and an assumed mean fuel molecular weight:

$$\left(\frac{Mass_{fuel}}{Mass_{air}}\right) = \frac{\left(ppmC_3H_8 \times 10^{-6}\right)\left(C_{ratio}\right)\left(MW_{fuel}\right)}{MW_{air}} \qquad (2.2)$$

where C_{ratio} was the carbon ratio, 3/9.58, and the average molecular weight of the fuel vapor used was 132.4. The author in ref [2] made it clear that since the molecular weight of JP-8 used was an average value was only an estimate, the conversion to FAR did not reflect the exact value in the tank, but was more a generalization and can be used to show relative FAR.

These experimental setups proved very useful in the design stage of the experimental process. Both experiments provided necessary insight into designing a fuel tank experiment instrumented with temperature, pressure, and hydrocarbon measuring devices, and provided methods of varying environmental conditions in the experiment.

3.0 EXPERIMENTAL APPARATUS

All experimentation was performed at the William J. Hughes Technical Center at Atlantic City Airport, New Jersey, with the support and supervision of the Fire Safety branch of the Federal Aviation Administration's research and development division. An experiment was designed to study the effects of varying ambient conditions on ullage vapor concentration and to make the data available for validating model calculations. This was accomplished using an experimental fuel tank that could contain any mass

loading of fuel and be subjected to varying fuel, surface, and ambient temperatures and sub-atmospheric pressures. Temperature, pressure, and overall vapor concentration data were recorded during experimentation and input into the computer model to compare the predicted values with the experimentally obtained results.

The fuel tank, shown in figure 3.1, was constructed of ¼" aluminum metal sheets welded together into a cube with outer dimensions 36" wide by 36" deep by 24" high. Two access panels measuring 12" wide by 18" deep were located on the top surface to allow for thermocouple pass-thru and ullage sampling. 2" and 3" diameter holes are also located on the top surface, one for fuel fill and the other to allow for ullage venting during ambient pressure changes. The tank was on a 2' high stand to allow for the fuel to drain out easily through a hole in the bottom surface. The tank was inside an environmental chamber, shown in figure 3.2, with inner dimensions 6' wide by 6' high by 8' deep. The chamber had the capability of varying the temperature and pressure with a cascade-type air conditioning unit that could drop the temperature as low as -100°F and a vacuum pump that could drop the pressure as low as about 2 psia. Micristar-brand temperature and pressure controllers located in the control booth had the capability to program in test-specific profiles for the temporal temperature and pressure variations.

12 Omega Engineering K-type thermocouples were located in various places throughout the tank and chamber; 8 were 1/16" flexible thermocouple probes and 4 were surface mountable thermocouples to measure the tank surface temperatures. 4 thermocouples were located in the liquid fuel, one of which was used by the heater temperature controller to maintain a specified liquid temperature, 3 more were located in the ullage, and 1 was in the ambient chamber air. All thermocouples had an accuracy of

±1°F. A Brisk Heat 2,160 watt silicone rubber heating blanket measuring 36” x 36” was mated to the bottom surface using RTV high temperature adhesive. An Omega Engineering CN616 series 6-channel temperature controller limited the blanket temperature. It had the capability to control the ramp up to a specified temperature and maintain that within a few degrees.

Total hydrocarbon concentration within the ullage space was measured using a flame ionization detector (FID) hydrocarbon analyzer. A Model VE7 heated total hydrocarbon analyzer by J.U.M. engineering, shown in figure 3.3, was the analyzer used in the experiments. FID’s can detect the concentration of hydrocarbons in a sample by burning the sample in a hydrogen flame. When the sample is introduced into the hydrogen flame an ionization process is initiated that releases free ions. An electrostatic field is created by a high polarizing voltage applied to two electrodes near the burner. Positive ions collect at the high voltage electrode and negative ions migrate to the collector electrode. The current generated between the two electrodes is directly proportional to the amount of hydrocarbons in the sample, and provides accurate total hydrocarbon measurements in terms of a volumetric concentration relative to the calibration gas, in this case propane.

The burner oven is heated to 374°F so that no condensation of fuel vapor occurs before reaching the flame. It is for this reason that heated sample lines and a sample pump with heated heads were required to draw the sample from the tank to the analyzer. Two Technical Heaters heated lines were used, 14’ and 4’, and maintained at 300°F by Technical Heaters temperature controllers. An Air Dimensions, Inc. Dia-Vac dual heated head pump was used to draw samples from sub-atmospheric pressures, as the FID’s built-in sample pump could not maintain the required sample pressure for tests at low ambient

pressures. The heaters in the pump heads were maintained at 300°F by the Omega 6-channel temperature controller. The FID required a 40% hydrogen / 60% helium fuel gas, and was calibrated with 2% propane in a nitrogen balance and checked for linearity with 4% propane in nitrogen, while hydrocarbon-free "zero" air or nitrogen was used to zero the analyzer. The output of the analyzer was in parts per million (ppm) propane equivalent on a scale of 0 to 100,000 corresponding to 0 to 10 volts DC output.

The FID had the following measured characteristics: a response time of 0.2 seconds, a maximum sensitivity of 0.1 ppm CH_4 in the lowest range, a zero and span drift of <1.0% of full scale in 24 hours, and linearity within 1% of the selected range. The measurement uncertainty was calculated using the procedure outlined in reference 24. The resolution of the FID was scaled to the measurement range used in the experiments as:

$$resolution = \frac{0.1\,ppm}{10\,ppm} * 100{,}000\,ppm = 1000\,ppm \qquad (3.1)$$

The *zero-order* uncertainty is arbitrarily assigned a numerical value of one-half of the FID resolution at the measurement range used:

$$u_0 = \pm\frac{1}{2} resolution = \pm 0.5 * 1000\,ppm = \pm 500\,ppm \qquad (3.2)$$

The RSS (root-sum-square) method was used to determine the combined instrument error. The listed instrument error factors from the manufacturer datasheet are the zero drift, span drift, and linearity over the measurement range. Therefore, using the RSS method, the instrument error is:

$$u_c = \pm\sqrt{zero_{drift}^2 + span_{drift}^2 + linearity^2} \qquad (3.3)$$

The zero and span drift are given in % per day, but all tests were less than one day, and the maximum test time was about 12,000 seconds, or three hours and twenty minutes. Therefore, the zero and span drift error per test could be given as:

$$zero_{drift} = span_{drift} = 3\frac{1}{3} hours * \frac{1.0\% * 100{,}000\, ppm}{24 hours} \cong 138 \frac{ppm}{test} \quad (3.4)$$

The linearity error was calculated as:

$$1.0\% * 100{,}000\, ppm = 1{,}000\, ppm \quad (3.5)$$

So the overall instrument error was determined to be:

$$u_c = \pm\sqrt{2 * 138^2 + 1{,}000^2} \cong \pm 1{,}018\, ppm \quad (3.6)$$

The design stage uncertainty could then be calculated as:

$$u_d = \sqrt{u_0^2 + u_c^2} = \sqrt{50^2 + 127^2} \cong \pm 1{,}134\, ppm \quad (3.7)$$

This level of error was accepted as suitable for the measurements being made in these experiments.

All data was collected on a PC by means of a data acquisition system. The software was designed and setup by in-house computer engineers at the technical center. The data was saved on the PC and could easily be exported to a spreadsheet for data processing.

Figure 3.1. View of top surface of fuel tank. Heated sample lines are the black hoses connected to the sample panel.

Figure 3.2. View of the fuel tank inside the environmental chamber. The fuel drums used for fill and drain are in the foreground. The control booth is to the right of the chamber.

Figure 3.3. View of the instrumentation rack. From top to bottom are: Pressure transducer display, span gas manifold, hydrocarbon analyzer, temperature controller panel, and heated sample pump.

4.0 EXPERIMENTAL PROCEDURE

The overall purpose of this research was to generate a set of data that can be used for validation of fuel vaporization model calculations. Therefore, the testing procedure was designed around the needs of the assumptions made in the model used in this work [11]. The starting conditions for each experiment were critical to the calculations, and for this experimentation it was decided to begin each test after sufficient equilibration of the system. This was typically achieved one or two hours after the fuel has been loaded into the tank and allowed to sit in the closed environmental chamber. The data obtained from the experiments, explained later, indicate that the temperatures were uniform throughout

the tank and the ullage vapor concentration was varying very little with time. This quasi-equilibrium was critical to the calculations, as it was necessary to have a starting condition where the ullage vapor concentration was nearly steady, known, and could be determined with equilibrium calculations. Subsequent time-marching calculations initiated with the equilibrium calculation, so it was imperative to have a correct assessment of the equilibrium condition. The system was considered steady if the ullage vapor concentration varied by less than 1,000 ppm or 0.1% over a period of ten minutes. At this quasi-equilibrium stage, the mass balance dictates that the rate of fuel vaporizing is equal to the rate of fuel condensing, and the amount of fuel in the ullage is constant.

In order to obtain accurate readings with the FID hydrocarbon analyzer, a lengthy warm-up procedure is recommended by the manufacturer. Since the warm-up typically takes about 4 or 5 hours, the analyzer was usually turned on Monday morning and allowed to run until the end of the week. The warm up procedure started with turning on the burner oven heater and allowing the temperature to stabilize at 190°C for one hour. At this point the sample pump was switched on and allowed to run for 30-45 minutes, after which time the flame could be lit by purging the fuel and sample lines for 1 minute, then pressing the igniter button. After the burner was lit, a stabilization time of 2-3 hours was required before the analyzer would be accurate. Hydrocarbon-free “zero” air or nitrogen (whichever was available) was passed through the analyzer for about 15 minutes to set the zero hydrocarbon concentration, then the 2% propane was passed through to set 20,000 ppm. Linearity was checked by passing through 4% propane to see if the analyzer read 40,000 ppm. This linearity check allowed for a hydrocarbon concentration range accurate from 0 to 40,000 ppm, which was enough for most of the testing involved.

The fuel used in this experimentation was obtained from the Atlantic City International Airport and delivered via fuel truck to the laboratory. Ten fuel drums were filled with JP-8, sealed and stored outside the laboratory due to technical center safety regulations. One fresh fuel drum was allowed to be stored in the lab while testing, and one was allowed in the lab to drain fuel into from completed tests. When the used fuel drum was full, it was dumped into large underground fuel tanks outside the laboratory. The fuel was then re-used by the jet engines that power the wind tunnel at the Air Induction Facility, which is at the same location as the laboratory, since the fuel has only been heated and not combusted or tainted in any way. Throughout the testing, two fuel samples were taken from fresh drums and stored in 500 ml bottles, once in the beginning of the series of tests and once at the end. The samples were sent over to the Fuels Research Facility at the technical center for a flash point test. The results from the tests are shown in the appendix.

The tests performed are shown in the matrix presented in table 4.1. Besides some initial instrument calibration tests, the first tests run were primary validation tests at sea level to evaluate the model's calculations with as few variables as possible. Initially, tests were run without fuel in the tank to confirm the energy balance in the model by comparing the measured and calculated ullage temperature profile. A single component fuel, isooctane (99.9% reference grade 2-2-4 trimethylpentane), was used to compare the measured and calculated fuel vapor composition without the ambiguity of the complex composition of JP-8. Testing with JP-8 was conducted as per the test matrix in table 4.1. A fuel quantity of 5 gallons, corresponding to a liquid layer thickness of 2.28 cm (0.9") and mass loading of 31.5 kg/m^3, was used for each test. Lower fuel loadings were

attempted, but provided inaccurate fuel temperature measurements due to the decreased thickness of the liquid layer, causing fuel puddles to form in some regions and an uneven liquid layer distribution. Initially, the fuel temperature set point was to be used as a variable in the matrix; however, fuel temperatures above 125°F were found to create vapor concentrations beyond the calibration range of the FID. Therefore, the fuel temperature set point was generally 30°F higher than the equilibrium fuel temperature, as it was found sufficient to demonstrate vapor evolution from a heated liquid without exceeding the FID calibration range. Several experiments were performed for each location in the test matrix to verify the repeatability of the experiment.

Table 4.1. Test Matrix

	Altitude			
Test Type:	***0***	***10,000***	***20,000***	***30,000***
Const. P	**X**	**X**	**X**	**X**
Vary T & P	*N/A*	**X**	**X**	**X**
Isooctane	**X**	*N/A*	*N/A*	*N/A*
Dry Tank	**X**	*N/A*	*N/A*	**X**

4.1 Constant Pressure Tests

The fuel was loaded into the tank and allowed to equilibrate for at least 1-2 hours, as this length of time was determined sufficient for equilibrium. During equilibration the heated lines were switched on and the hydrocarbon analyzer was zeroed and calibrated with 2% and 4% propane mixtures. The fuel temperature set point was dialed into the blanket heater temperature controller and the test-specific settings were loaded into the DAS. After sufficient time was allowed for equilibrium to be attained, the DAS was set to begin sampling and the hydrocarbon analyzer sample location was switched from ambient air outside the chamber to inside the fuel tank. After a few minutes of recording temperature

and hydrocarbon data at equilibrium, the tank heater was switched on. The DAS took samples every 2 seconds while the test operator manually wrote down temperatures and hydrocarbon concentration on test data sheets every ten minutes. The test was allowed to run until the hydrocarbon concentration became quasi-steady, or no increase in concentration larger than 1,000 ppm over ten minutes. It was determined in previous work [2] that this rate of change could be considered quasi-steady equilibrium. After the test was completed the tank heater was turned off and the fuel was allowed to cool to room temperature before being pumped out of the tank. The DAS was stopped and the data was saved and exported.

The procedure for the dry tank tests was similar except no fuel was used; therefore no hydrocarbon data was recorded. The tank was heated and allowed to reach quasi-steady thermal equilibrium while recording all temperatures. Isooctane tests were identical to JP-8 tests except that the isooctane needed to be cooled to well below room temperature to about 5°F in order to obtain fuel vapor concentrations within the calibration range of 0-40,000 ppm, since isooctane is much more volatile than JP-8. Equilibrium was attained at these lower temperatures after 1-2 hours; then the test procedure described for JP-8 was followed. The constant sub-atmospheric tests were also similar except that the pressure was initially dropped after the fuel was loaded. Equilibrium was attained after 1-2 hours at decreased pressure, then the fuel was heated and samples were taken.

The FID’s built-in sample pump was only designed to draw samples from atmospheric pressure, so in order to sample from sub-atmospheric pressures an auxiliary pump was required. The sample pump chosen was a dual heated head high flow sample

pump that could draw samples from altitudes as high as 35,000 feet. However, when sampling from altitudes lower than 35,000 feet, the pump would draw more than the necessary amount required by the FID, which would just be wasted by dumping into the laboratory air. Also, by drawing a continuous sample at a high flow rate, hydrocarbon-free air would be drawn in to the ullage through the vents, which would dilute the sample and cause the FID readings to be false. It was for these reasons that an intermittent sampling method was devised for tests to be performed at sub-atmospheric pressures. The FID had a very high response time of 0.2 seconds, so a sample time of 30 seconds every ten minutes was agreed upon taking into consideration the analyzer response time, the flow rate of the sample pump and the length of the sample lines.

4.2 Flight Profiles

A flight profile is the temporal pressure and temperature variation for the duration of the test. Before a flight profile test was run the fuel was loaded into the tank and allowed to equilibrate. A flight scenario was created that simulated an airplane on the ground for about an hour at ambient sea level temperature and pressure with heating of the fuel tank to about 30°F above the initial liquid temperature. Quasi-steady equilibrium was attained after about an hour, then the airplane began ascent at 1,000 feet per minute until the cruising altitude was reached. The airplane would cruise at altitude for an hour then begin decent at –1,000 feet per minute. The test was complete after the airplane was back on the ground. Ambient temperatures at high altitudes were obtained from Unisys weather constant height plots. Ambient temperatures of 20°F, -10°F, and -50°F were used at altitudes of 10,000 feet, 20,000 feet, and 30,000 feet, respectively. A linear

variation for the ambient pressure and temperature was calculated for each test and programmed into the chamber controllers at the beginning of each test. After equilibrium, the flight profile was initiated and the fuel tank heater was switched on. Samples were taken intermittently every ten minutes using the heated sample pump. The test was terminated when the flight scenario was finished and the data was saved and exported.

4.3 Model Calculations

The data from all tests was exported from the test computer onto a desktop PC. The files were converted into text files and loaded into Visual Fortran. The fuel properties obtained from reference 20, such as mole fractions of C5-C20 compounds and their corresponding boiling points and densities, were loaded in as inputs, as well as the coefficients from Wagner's equations [28]. As was previously mentioned, two fuel compositions from ref [20] were used for the calculations with flashpoints of 115°F and 120°F in order to bracket the test fuel flashpoint of 117°F.

5.0 RESULTS

When inputting the experimental data into the computer model, it was important to adjust the pressure profile so that it is near constant or changing at a constant rate. This is due to the fact that the pressure transducer output varied by about 0.002 psia per sample, which would cause minor fluctuations in the readings. The model calculations are sensitive to pressure, as it is the pressure difference that is used to calculate the venting of ullage vapor out of the tank and the inflow of air into the tank. If the pressure at the subsequent time step is less than the previous time step, the model calculates venting of ullage vapor out of the tank. If the pressure at the subsequent time step is greater than the previous time step, the model calculates there will be an inflow of air into the ullage, diluting the ullage vapor mixture. It is for this reason that although the pressure fluctuations may balance out around the actual pressure, the model will calculate that ullage vapor will leave the tank while only air will return to the tank, effectively reducing the ullage vapor concentration as time goes on. This was done for both constant and varying ambient pressure tests. For constant pressure tests, an average of the pressures recorded during the test was used as the constant pressure. For varying ambient pressure tests, linear interpolation was used to obtain constant linear variation in pressure from an initial to a final pressure. Figure 5.0 shows the measured and adjusted pressure, including the relations used for adjusting the pressure profile, for a simulated flight up to 30,000’ cruise.

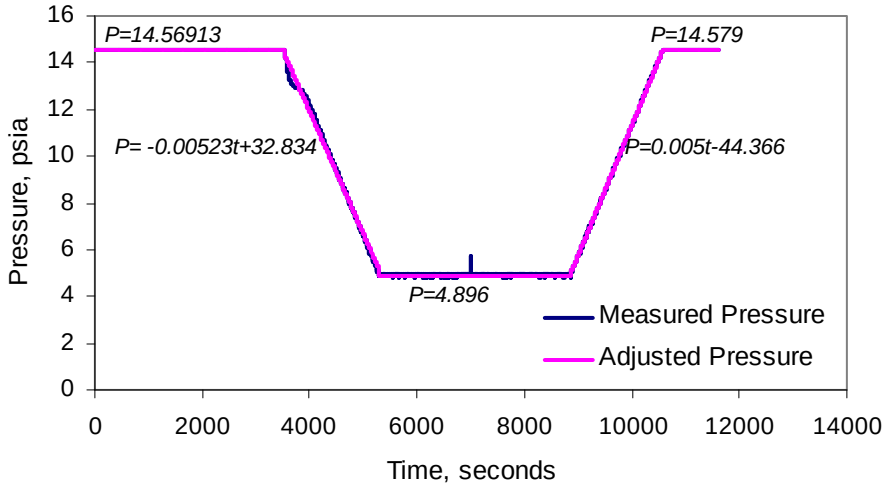

Figure 5.0. Measured and adjusted pressure profiles for a 10,000' altitude flight profile test.

5.1 Validation Tests

5.1.1 Tank Mixing

Results with a dry tank test at 30,000' altitude (4.6 psia) are displayed in figure 5.1, showing the lower tank surface temperature and the measured ullage temperatures from the three thermocouples located at different positions in the ullage. Similar results are shown in figure 5.2 for a tank at sea level ambient pressure containing liquid fuel at a loading of 31.5 kg/m^3. The results in figures 5.1 and 5.2 are typical of all of the data and show that all three ullage thermocouples measured about the same value or within the measurement error of ±1°F. This confirmed that the bulk ullage gas in the test tank was well mixed due to the turbulent natural convection within the tank.

Figures 5.3 and 5.4 show a comparison of the mean measured ullage temperature (average of the three ullage thermocouple measurements) with the ullage temperature predicted by the model in ref [11]. The good agreement, within approximately 2%,

between measured and predicted values is typical of the agreement for the remaining data sets, and serves as validation of the tank overall energy balance calculations in the model.

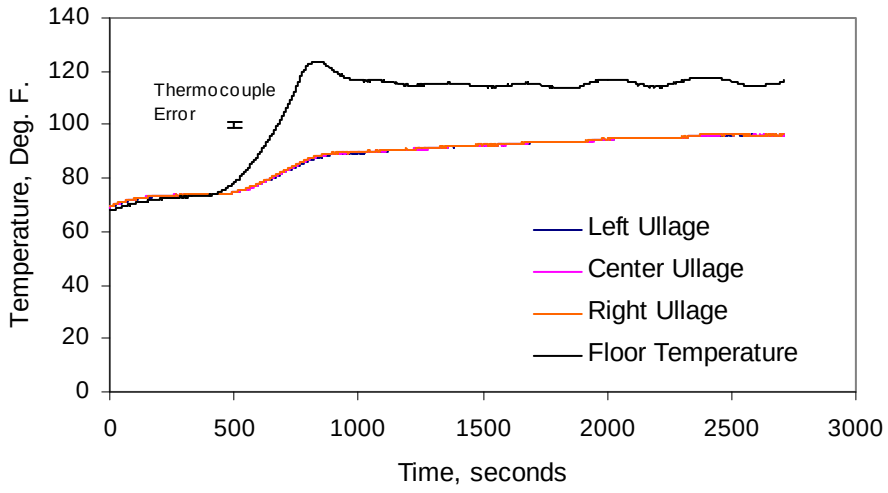

Figure 5.1. Measured ullage and floor temperature for a dry tank at 30,000' (4.6 psia).

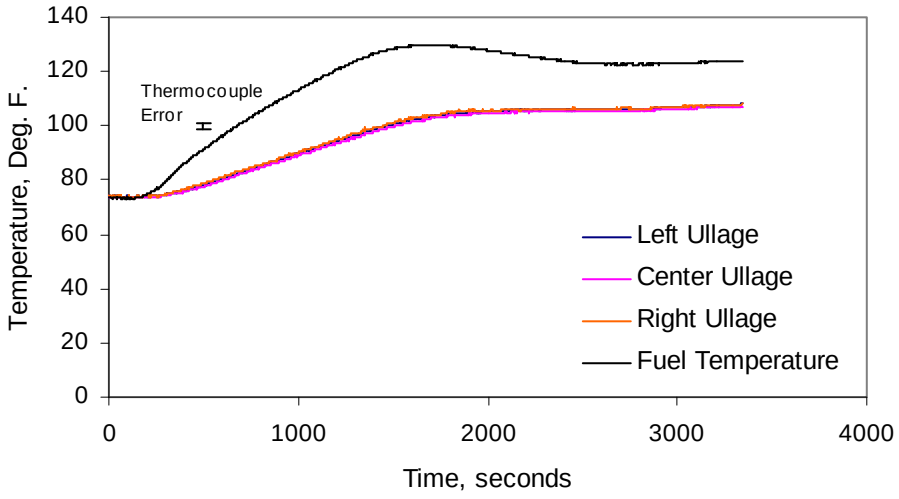

Figure 5.2. Measured ullage and fuel temperature for a partially filled tank (M.L.=31.5 kg/m^3) at sea level.

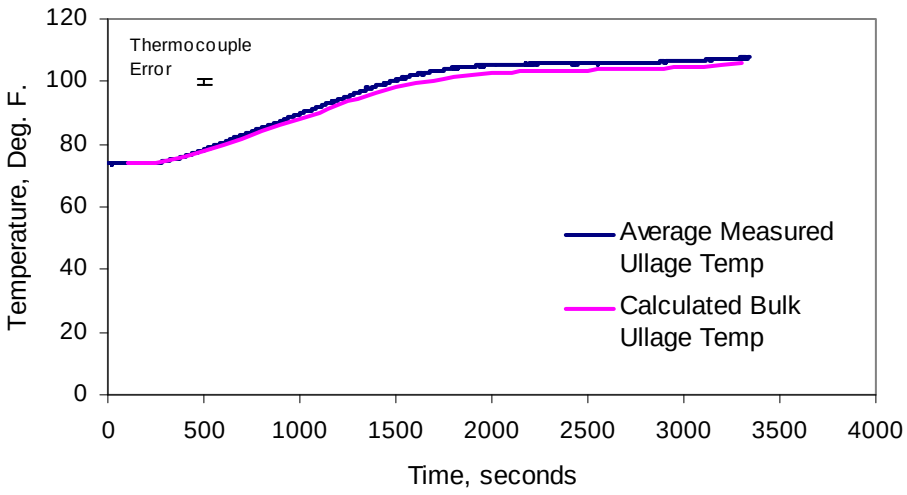

Figure 5.3. Measured tank temperatures and calculated ullage temperatures for a dry tank at 30,000' (4.6 psia).

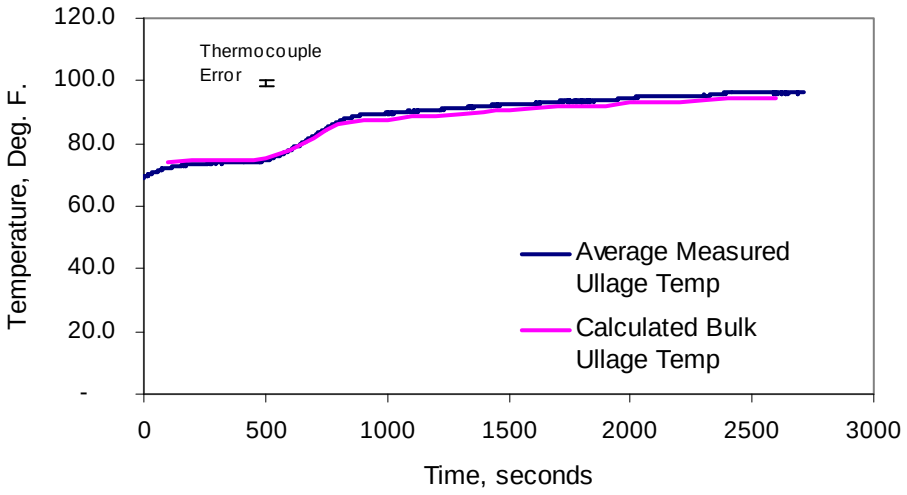

Figure 5.4. Average measured ullage temperature and calculated bulk ullage temperature for a partially filled tank (M.L.=31.5 kg/m^3) at sea level.

5.1.2 Isooctane Fuel Vaporization Test

Figure 5.5 shows results from single component fuel vaporization at atmospheric pressure and reduced ambient temperature. Isooctane being quite volatile, it was necessary to allow the fuel to cool for several hours to near 3°F in order to obtain fuel vapor concentrations within the FID calibration range of 0-4% propane equivalent. Figure 5.5 shows that at the start of the test, after cooling, there was very good agreement between the measured and calculated vapor concentration. As the fuel temperature increased, the ullage vapor concentration also increased due to increasing vaporization. The fuel vapor measurement was carried out intermittently at some times during the test to preserve the purity of the sample, as the test time was almost 2 hours. During the latter part of the test the FID vapor concentration measurements fluctuated at high vapor concentrations above 30,000 ppm. This was later seen in other experiments at high vapor concentrations as well, and was most likely due to some condensation occurring in the sample lines at cold spots and subsequent vaporization at warmer locations. Considering the difficulties involved in using isooctane as the test fuel, the agreement between the measured and calculated fuel vapor concentrations was considered satisfactory.

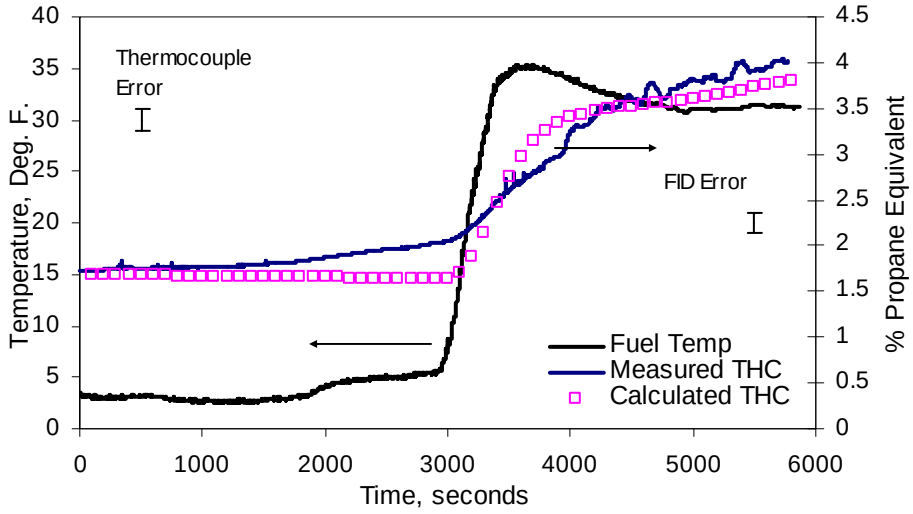

Figure 5.5. Isooctane fuel vaporization at atmospheric pressure and reduced ambient temperature, M.L.=31.5 kg/m^3.

5.2 JP-8 Tests at Constant Ambient Pressure

5.2.1 Atmospheric Pressure

Figures 5.6 and 5.7 show experimental and computed results at constant (atmospheric) pressure, for two tests with similar liquid fuel heating profiles. As was previously mentioned, the computed results were for two different fuel compositions (115°F and 120°F flashpoint from ref [21]) with flashpoints bracketing the measured test fuel flashpoint of 117°F. There was good agreement between experimental and calculated results, as the calculated ullage vapor concentrations using the two different fuel compositions bracketed the measured ullage vapor concentration. Likewise, figure 5.8 shows the results from the intermittent sampling test. Good agreement is again found between the calculated and measured ullage vapor concentrations.

It was necessary to compare the methods to determine if intermittent sampling could be used in the place of continuous sampling when necessary; i.e., at simulated high altitudes. Unfortunately, the comparison of the two methods couldn't be performed at

higher altitudes, as continuous sampling with the high flow sample pump would cause false readings by the FID due to air entering the ullage through the vents, and continuous sampling with the FID's built-in pump would not draw enough sample for the FID to give accurate readings. Therefore, the comparison was performed at sea level, where the continuous sampling with the FID's built-in pump was known to be accurate.

The two tests were intended to be identical, but varied slightly due to different initial conditions. Figure 5.9 compares the liquid fuel temperatures and measured vapor concentrations for the two tests. Considering the differences between the test conditions for the two tests, there is good agreement between the two methods of ullage vapor sampling, indicating that minor difference is noticed between intermittent and continuous ullage vapor sampling; thus, intermittent sampling can be used in lieu of continuous sampling when necessary.

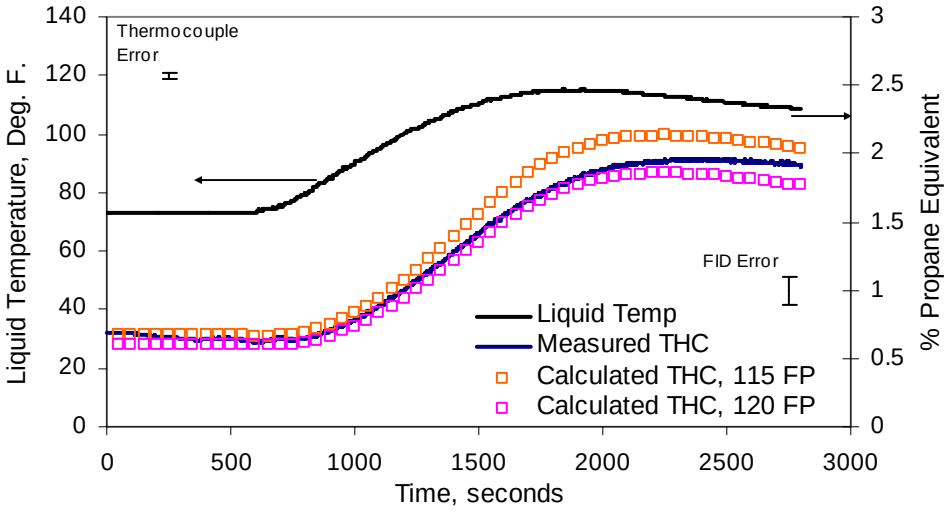

Figure 5.6. JP-8 fuel vaporization at sea-level, constant ambient pressure and temperature; comparison of calculated and measured ullage vapor concentration, M.L. =31.5kg/m^3.

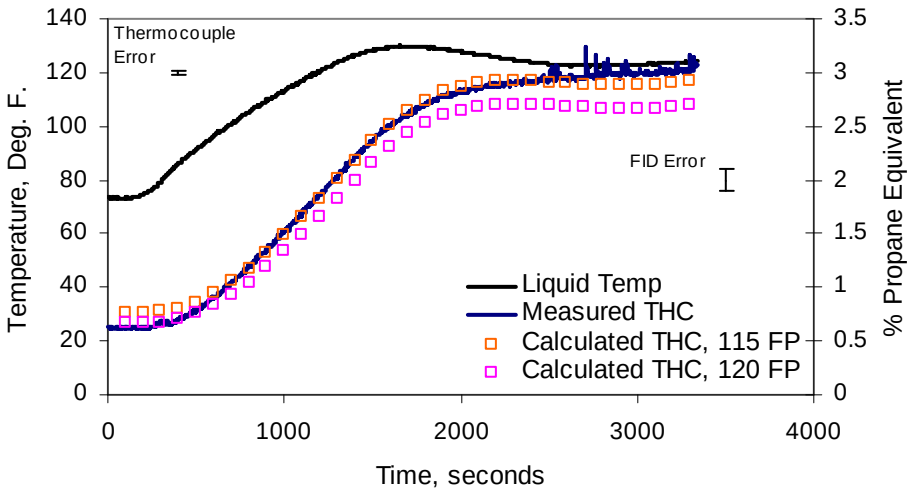

Figure 5.7. JP-8 fuel vaporization at sea level, constant ambient pressure and temperature; comparison of calculated and measured ullage vapor concentration (similar to previous test with higher final liquid temperature), M.L.=31.5 kg/m^3.

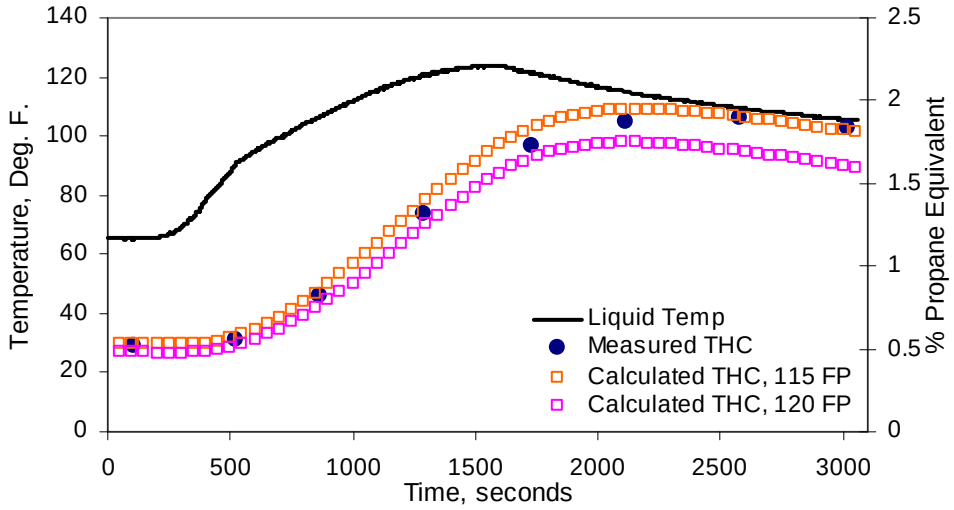

Figure 5.8. JP-8 fuel vaporization at sea level, constant ambient pressure and temperature; comparison of calculated and measured ullage vapor concentration with intermittent ullage vapor sampling, M.L.=31.5 kg/m^3.

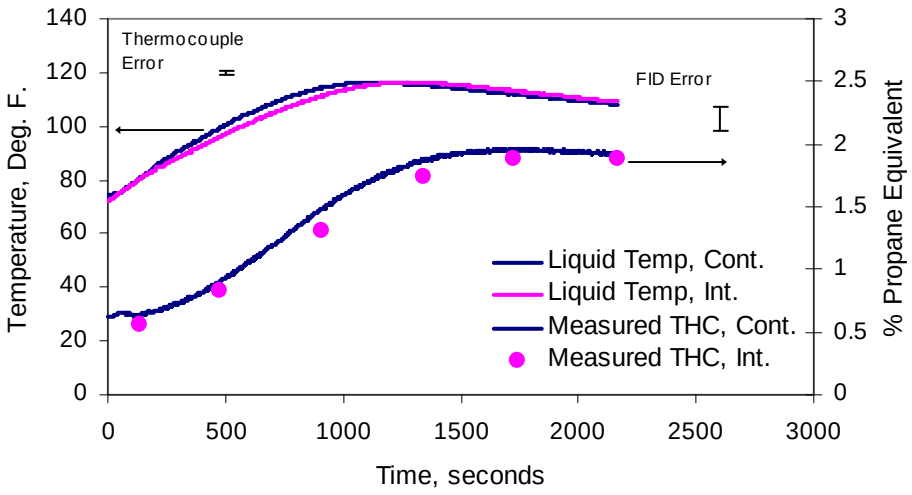

Figure 5.9. Comparison of continuous and intermittent sampling with two different JP-8 tests with similar heating profiles, M.L.=31.5 kg/^{3}.

5.2.2 JP-8 Tests at Reduced Constant Ambient Pressures

Three different tank pressures, 10.2 psia, 6.9 psia, and 4.6 psia, corresponding to standard atmosphere altitudes of 10,000', 20,000', and 30,000', respectively, were tested to determine the effect of decreased ambient pressure on fuel vaporization and on the predictions made by the model. The results in figures 5.10 and 5.11 were obtained with similar liquid fuel heating profiles starting at approximately 85°F, while the liquid fuel in the test displayed in figure 5.12 was initially cooled to approximately 40°F. As can be seen in the figures, good agreement is again found between the measured and calculated ullage vapor concentrations since the computed results for the two fuel specifications bracketed the measured data. As the altitude increased the concentration of fuel vapor in the ullage increased due to decreased air density at the reduced ambient pressure. At 30,000' altitude (with an ambient pressure of about 4.6 psia) the resulting fuel vapor concentrations exceeded the hydrocarbon analyzer's calibration range of 0-4% propane.

For the 30,000' altitude data, the chamber was therefore initially cooled so that the initial fuel temperature was about 40°F while the maximum liquid temperature was kept below approximately 60°F to reduce the fuel vapor pressure so that the ullage vapor concentrations remained within the calibration range.

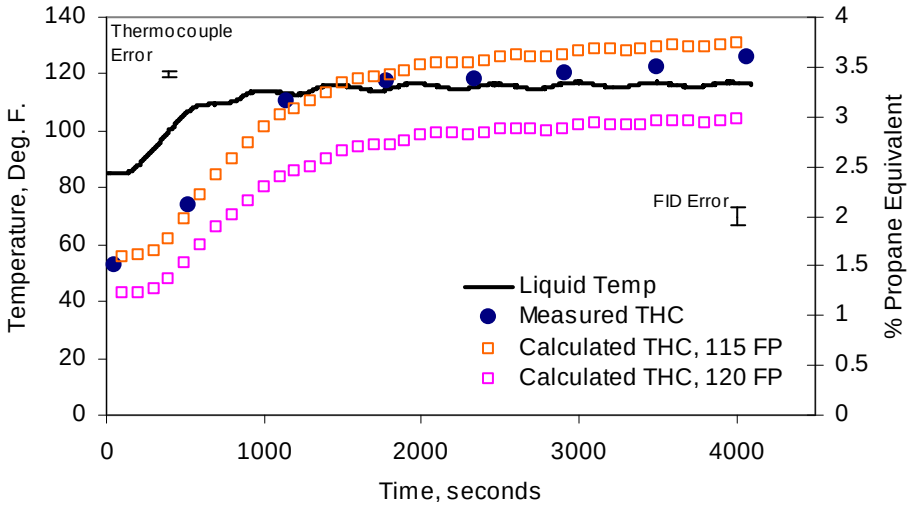

Figure 5.10. Fuel heating at 10,000' altitude, 10.2 psia; input fuel temperature and comparison of calculated and measured ullage vapor concentrations, M.L.=31.5kg/m^3.

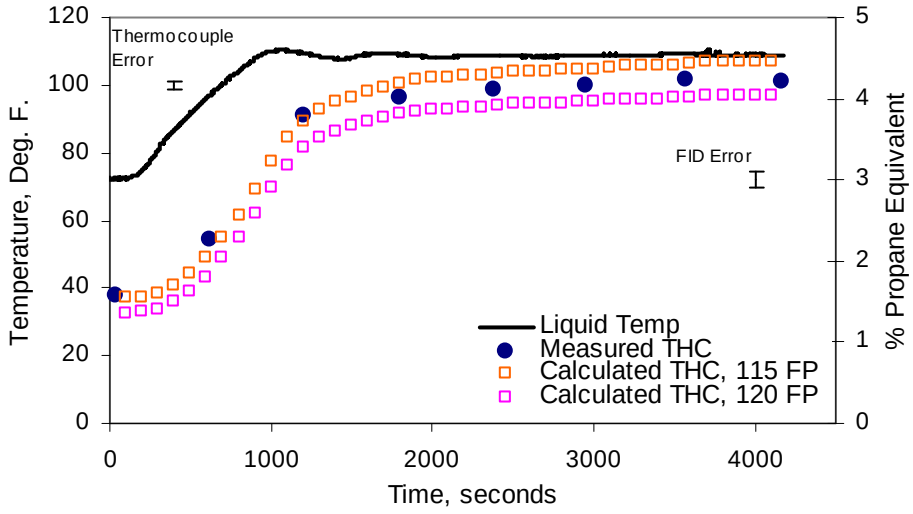

Figure 5.11. Fuel heating at 20,000' altitude, 6.9 psia; input fuel temperature and comparison of calculated and measured ullage vapor concentrations, M.L.=31.5kg/m^3.

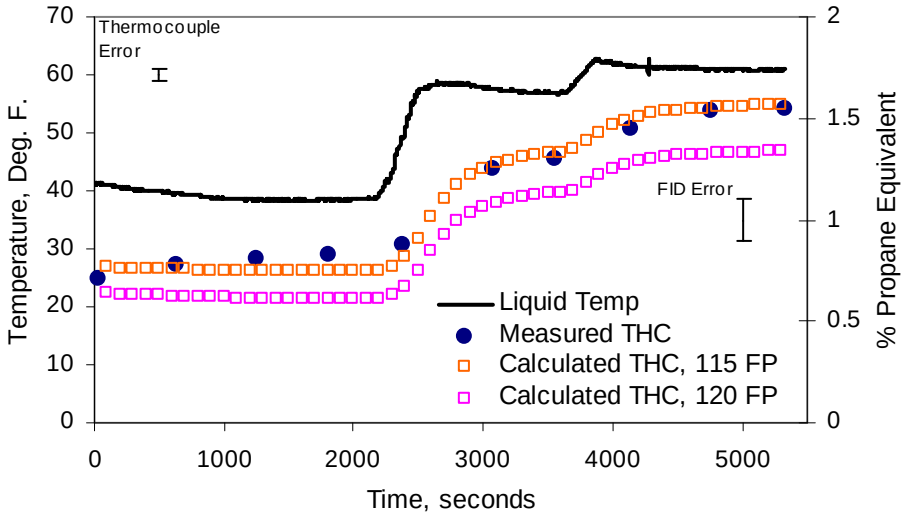

Figure 5.12. Fuel heating at 30,000' altitude, 4.6 psia; input fuel temperature and comparison of calculated and measured ullage vapor concentrations, M.L.=31.5kg/m^3.

5.3 JP-8 Tests with Simulated Flight Conditions

As mentioned earlier, simulated flight conditions consisted of one hour of ground time with fuel tank heating from the bottom surface, an ascent at 1,000 feet per minute to the desired cruising altitude (10,000', figure 5.12, 20,000', figure 5.14, 30,000', figure 5.16), cruise at this altitude for one hour, descent at –1,000 feet per minute to sea level, and finally several minutes at ground level. Ambient temperature profiles were based on weather data from Unisys constant height temperature plots of the United States. Although the conditions used in this part of the experimentation were not identical to the exact fuel tank conditions in an aircraft, they did provide a good indication of the conditions occurring during flight in a typical aircraft fuel tank. The results from the simulated flight profile tests, including the environmental flight conditions and ullage vapor concentration comparisons are shown in figures 5.12 – 5.17.

Figures 5.13, 5.15, and 5.16 show a comparison between calculated and measured ullage vapor concentrations for three flight scenarios with cruises at 10,000', 20,000', and

30,000', respectively. The same two fuel compositions with flashpoints of 115°F and 120°F were used for the calculations. As with the previously presented constant pressure data, the results show that the calculated vapor concentration profiles bracketed the measured vapor concentration profile, indicating that the model provided a reasonably accurate prediction of fuel vaporization under varying ambient conditions.

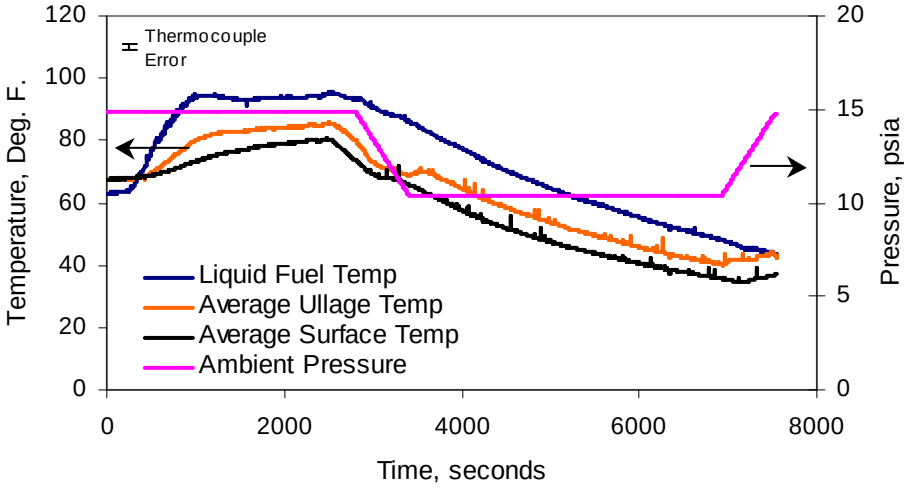

Figure 5.13. Test FLT-10: simulated flight with cruise at 10,000' altitude; fuel tank temperatures and ambient pressure.

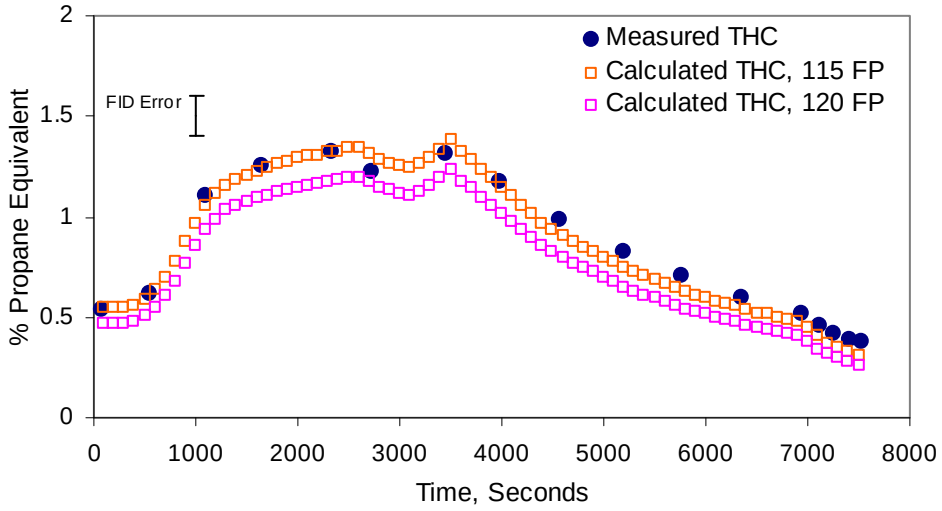

Figure 5.14. Test FLT-10: comparison of calculated and measured ullage vapor concentration for simulated flight with cruise at 10,000', M.L.=31.5kg/m^3.

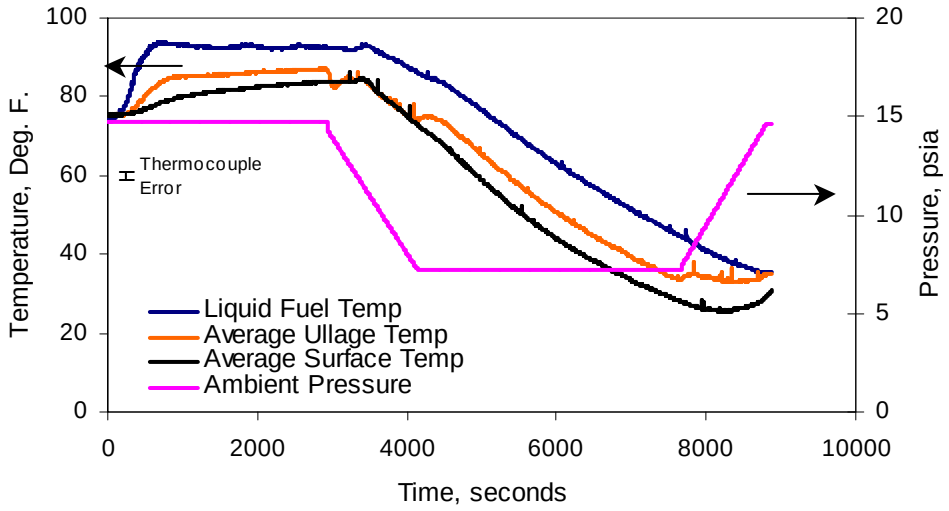

Figure 5.15. Test FLT-20: simulated flight with cruise at 20,000' altitude; fuel tank temperatures and ambient pressure.

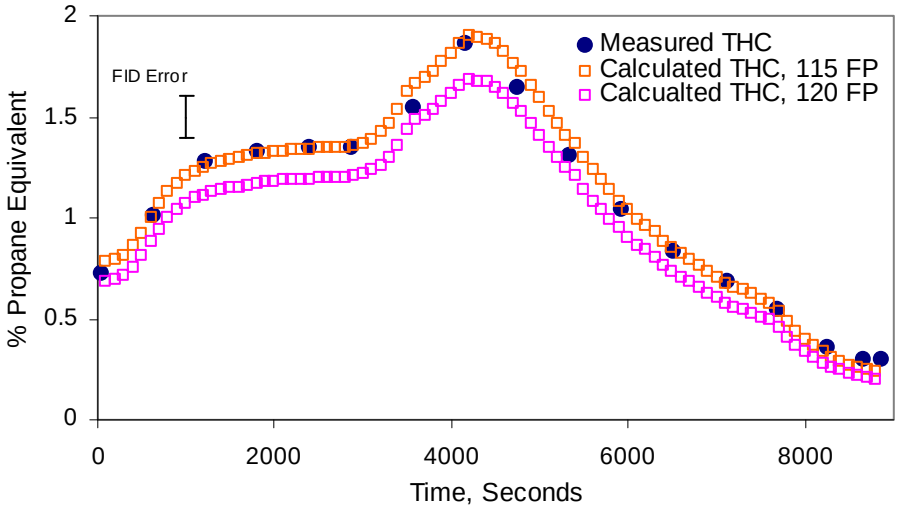

Figure 5.16. Test FLT-20: comparison of calculated and measured ullage vapor concentration for simulated flight with cruise at 20,000', M.L.=31.5kg/m^3.

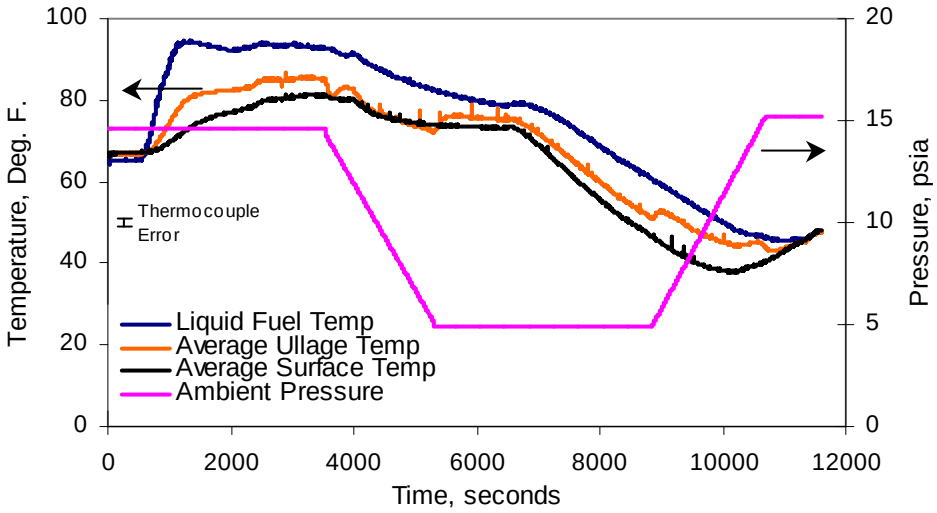

Figure 5.17. Test FLT-30: simulated flight with cruise at 30,000' altitude; fuel tank temperatures and ambient pressure.

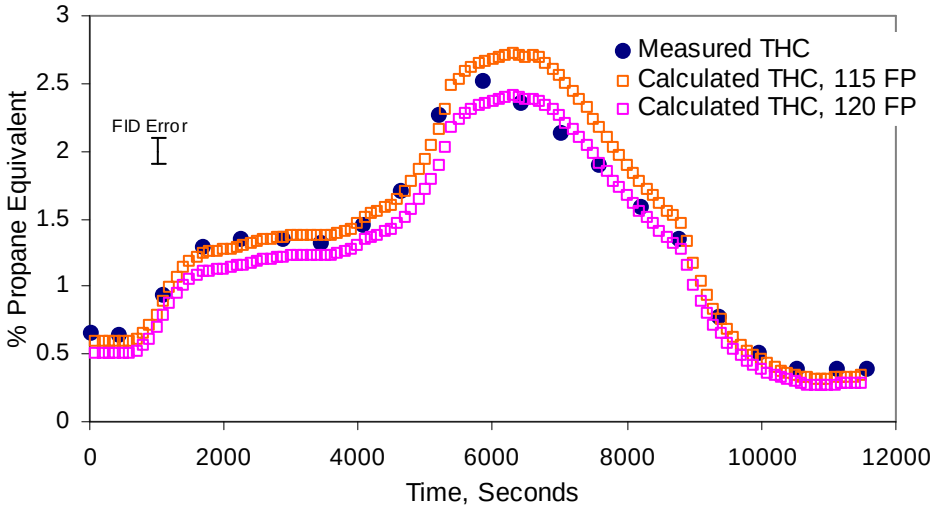

Figure 5.18. Test FLT-30: comparison of calculated and measured ullage vapor concentration for simulated flight with cruise at 30,000', M.L.=31.5kg/m^3.

6.0 DISCUSSION OF THE EXPERIMENTAL RESULTS USING MODEL PREDICTIONS

The model used in this work [11] was used to estimate the total ullage vapor composition by considering the vaporization of each of the species in the assumed fuel composition. Mass balances were used to determine the fuel stored in the ullage at a given moment considering the mass of fuel that has vaporized, condensed on the tank surfaces, and vented out of the tank. The calculated results can therefore be used to discuss the experimental data in terms of the overall mass transport occurring in the fuel tank within the limitations imposed by the *n*-alkane fuel characterization. The calculated composition of the ullage gas can also be used to estimate tank flammability using either Le Chatelier's ratio of the overall fuel to air mass ratio (FAR) criterion.

6.1 Calculated Mass Transport

6.1.1 Fuel Tank at Sea Level

The temporal variation of the experimental propane equivalent vapor concentration data can be discussed using the computed amount of vapor evaporated, condensed, and vented out of the tank. This will be demonstrated using two examples. The first example is the case of a heated fuel tank at sea level with constant ambient conditions, as presented earlier in figure 5.6; the second example is the test presented in figures 5.16 and 5.17, a simulated flight profile up to 30,000' altitude.

The measured data from the first example is presented again in figure 6.1, including the average fuel tank temperatures and measured total hydrocarbon concentration. Figure 6.2 shows the calculated temporal variation of mass of fuel evaporated, condensed, stored, and vented out. During the initial period of heating of the

liquid fuel the mass of fuel evaporated increased rapidly and was accompanied by an equivalent (except for the negligible mass vented) increase in the mass of fuel stored in the ullage. In addition, during part of this initial vaporization period the composition of ullage species was insufficient to satisfy dew point conditions on the tank walls, and as shown in figure 6.2, there was no condensation predicted until approximately 1800 seconds when such conditions were satisfied. As can be seen in figure 6.1, the liquid temperature was a maximum at approximately 1700 seconds. The gradual buildup of vapor species in the tank reduced the mass fraction difference between the liquid surface and the ullage gas, and hence the rate of vaporization. Together with the onset of mass removal by condensation, this resulted in a gradual reduction of the rate of increase of ullage vapor stored. Cooling of the liquid fuel further decreased the rate of vaporization and, as shown in figure 6.1, the mass stored eventually reached a maximum value at approximately 2200 seconds signifying a balance between the rates of vaporization and condensation. The mass stored then decreased continuously because of further cooling of the liquid fuel. As can be seen in figure 6.2 the mass of vapor vented out did not significantly affect the magnitude of the ullage mass.

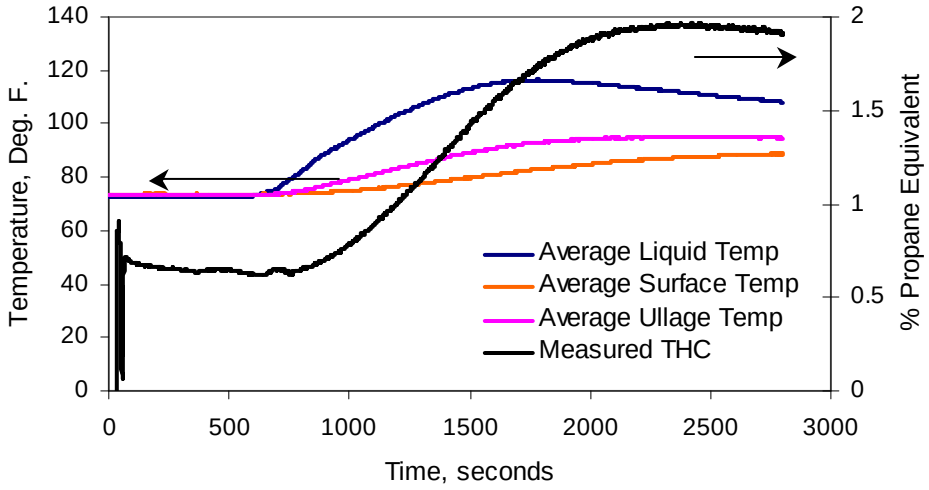

Figure 6.1. Average measured fuel tank temperatures and measured total hydrocarbon concentration for a heated fuel tank at sea level, constant ambient conditions.

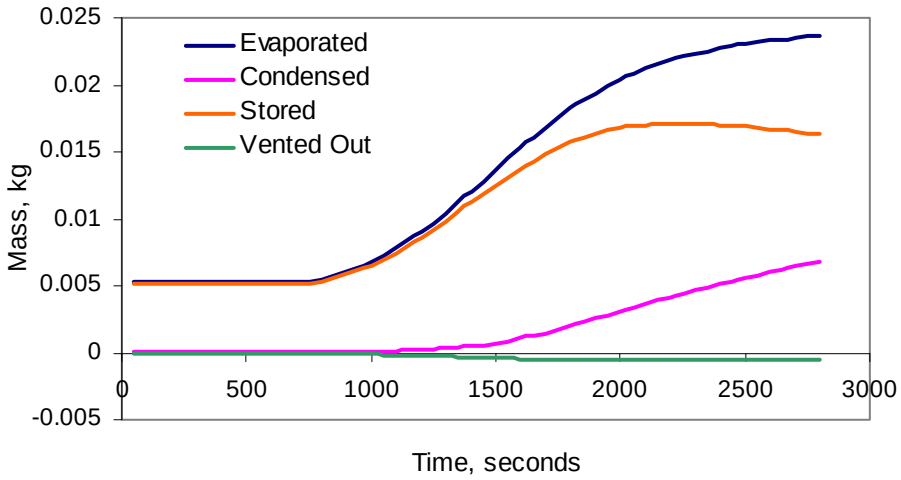

Figure 6.2. Calculated temporal mass transport occurring within the fuel tank for a heated fuel tank at sea level, constant ambient conditions.

6.1.2 Heated Fuel Tank Under Varying Ambient Conditions

Measured data for the second example, the case of an aircraft climbing, cruising, and descending from 30,000' altitude is shown in figure 6.3. Figure 6.4 shows the calculated temporal variation of the mass of fuel evaporated, condensed, stored, and vented out.

In the beginning of the test, the liquid fuel was heated to 30°F above its initial temperature and allowed to vaporize until quasi-equilibrium is achieved. From figure 6.4, it can be seen that the amount of fuel evaporated was similar to the amount of fuel stored in the ullage, because at this point there was little condensation. Once dew point conditions were reached, the condensation rate increased and the mass of fuel stored in the ullage leveled off even though the mass of fuel evaporated still increased, as it did for the duration of the test. As the climb to altitude was initiated, the mass of fuel stored in the ullage began to decrease rapidly as ullage gas was vented due to the pressure differential between the ullage and the atmosphere. The ambient air temperature was decreasing quite rapidly at this point due to the increasing altitude, and the fuel tank temperatures began to decrease, causing an increase in the rate of condensation and a decrease in the mass of fuel stored in the ullage. Upon descending from cruise, air entered through the vents due to the pressure differential and diluted the ullage vapor mixture. When the fuel tank was back to sea level atmospheric pressure, the fuel tank temperatures were about 15°F cooler than at the beginning of the test, and the mass of fuel stored in the ullage was about 0.002 kg less than at the beginning.

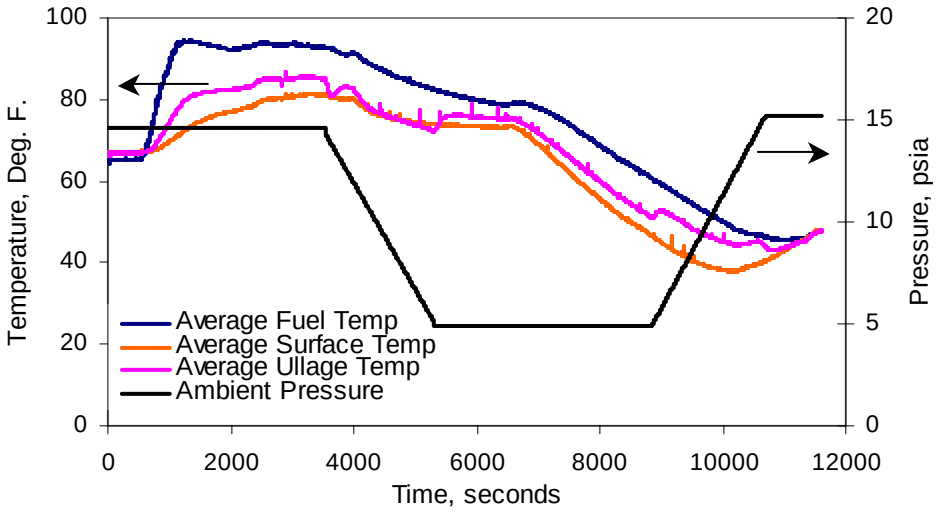

Figure 6.3. Fuel tank temperatures and ambient pressure for a flight profile test up to 30,000' altitude.

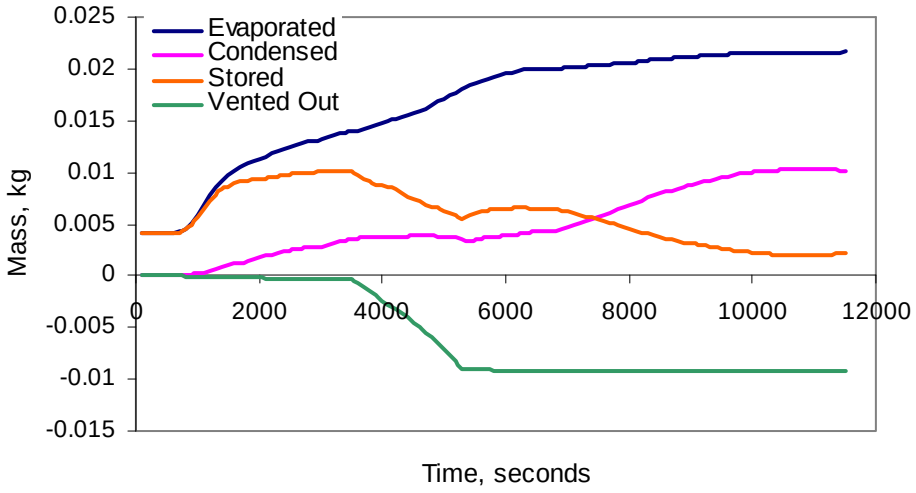

Figure 6.4. Calculated temporal mass transport occurring within the fuel tank for a flight profile test up to 30,000' altitude.

6.2 Flammability Assessment

6.2.1 Fuel Tank at Sea Level

Determination of the fuel to air mass ratio is important in fire hazard assessment because it can be compared with a lower flammability limit (LFL) of a combustible mixture. For multicomponent fuels, such as Jet A, it is not in general possible to identify a single LFL since the ullage vapor composition may vary with loading ratio, with the liquid temperature, and the time from initiation of heating. An approximate criterion used for estimating the FAR at the LFL is that at the LFL the FAR for dry air volume of most saturated hydrocarbons on a mass ratio basis is 0.035±0.004 at 0°C (32°F) [26]. This can then be used as an estimate of the FAR at the LFL since Jet A consists mainly of paraffinic saturated (75%-85%) hydrocarbons, and the results can be compared with FAR's computed in the present work since they are based on a straight chain alkane characterization of the fuel.

Figure 6.5 shows the calculated temporal change in FAR of the heated tank at sea level and the range of the FAR at the LFL using the two different fuel compositions. According to the estimate of the lower flammability limit [26], the mixture became flammable at about 1800 seconds, and from simultaneous inspection of figure 6.1, the average liquid temperature at that point was about 116°F, which was very close to the measured flashpoint of 117°F. By comparing the initial fuel temperature to the temperature at which the mixture was flammable, a fuel temperature rise of about 43°F was necessary to cause an initially non-flammable fuel tank to possibly become flammable.

The flammability of a mixture of a known (or assumed to be known) composition can also be determined using Le Chatelier's flammability rule [27], as described earlier in equation 2.1. The LFL of a multicomponent mixture can then be estimated by the relationship:

$$LC = (1.02 - 0.000721 * T) \sum_{I} \frac{x_i}{LFL_i}, i = 1 \rightarrow N \qquad (2.1)$$

where x_i is the mole fraction of species i in the mixture and LFL_i is the lower flammability limit (25°C) of species i. The mixture is considered flammable if LC>1. It is more explicitly stated here than for the FAR flammability rule that the flammability of a mixture is dependent upon not only the amount of fuel in the mixture but also the composition of the fuel vapor, as LC is calculated considering both the fraction and the LFL of each individual species in the mixture. Figure 6.6 shows the calculated Le Chatelier's ratio for the two fuel compositions with flashpoints of 115°F and 120°F. Le Chatelier's rule indicates that even the more volatile 115°F flashpoint fuel did not become flammable throughout the length of the test. From a safety standpoint, the FAR rule appears to be more conservative and indicates that mixtures may become flammable earlier than the Le Chatelier's rule does. Application to the present results obtained using equivalent fuel species characterizations requires additional consideration, including experimental verification, but for comparison purposes the computed fuel species mole fractions in the ullage, represented in terms of C5 to C20 normal alkanes only, were used with equation (1) to calculate the LC ratio as a function of time.

Figures 6.7 and 6.8 show calculated fuel to air mass ratios and Le Chatelier's ratio, respectively, using the input data from the first example (a heated tank at sea level), as well as two other profiles with liquid temperatures 5°F and 10°F higher than the

average measured liquid temperature to demonstrate the effect of fuel temperature on vapor generation. The original average measured liquid temperature profile is referred to as TLIQ and the other two profiles were obtained by adding 5°F and 10°F to TLIQ and are referred to as TLIQ+5 and TLIQ+10, respectively. The 115°F flashpoint fuel composition was used for these calculations as a worst-case scenario, as this fuel composition was demonstrated earlier to generate more vapors than a 120°F flashpoint fuel composition. Following the FAR flammability rule, the fuel tank was seen to become flammable much earlier in the test for higher liquid fuel temperature profiles, indicating the strong effect of fuel temperature on flammability. Similar, but more conservative results can be shown using Le Chatelier's rule in figure 6.8.

To study the effects of the amount of fuel in the tank on the flammability of the ullage, several calculations were made with the same data but varied the fuel mass loading. The experiments were conducted with five gallons of fuel in a 128 gallon tank, which is equivalent to a mass loading of 31.5 kg/m^3. The calculations of FAR and LCR were carried out with two additional mass loadings, 300 kg/m^3 and 0.5 kg/m^3, and the results are displayed in figures 6.9 and 6.10. It can be seen that the overall FAR and LCR decrease as the fuel loading is decreased, and that in order to have a significant effect on decreasing the flammability, the mass loading needs to be lowered to an extremely low value (0.5 kg/m^3) which is essentially an empty fuel tank with a very thin film (0.001" thick) of residual fuel across the bottom surface. This agrees with the conclusions made in previous experimental studies of mass loading effects on flammability [2].

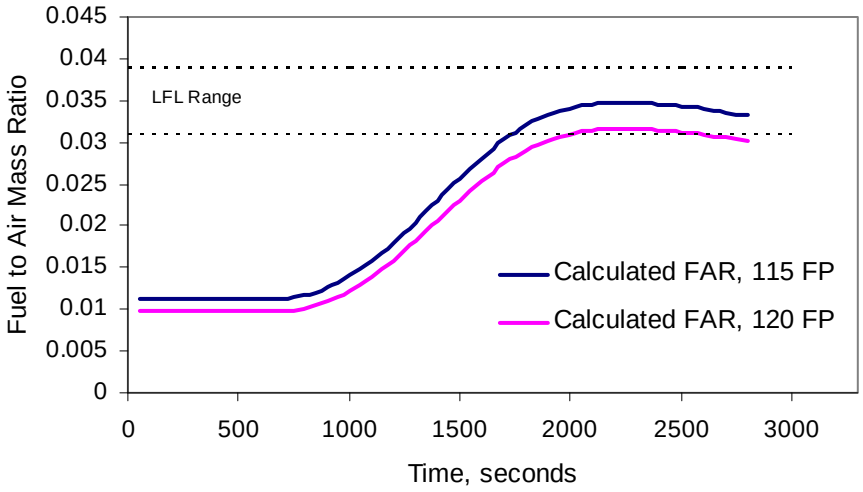

Figure 6.5. Temporal change in FAR for a heated fuel tank at sea level with constant ambient temperature and lower flammability range [26].

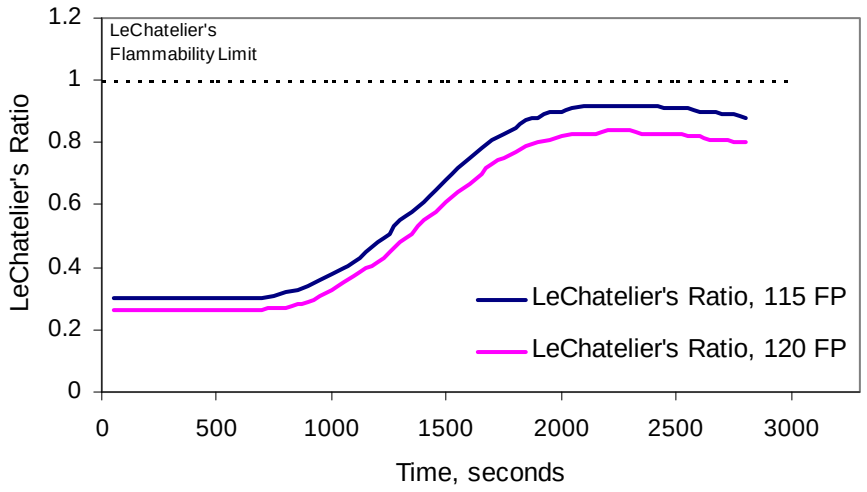

Figure 6.6. Temporal change in calculated Le Chatelier's ratio calculated for two fuels with flashpoints of 115°F and 120°F for a heated fuel tank at sea level and Le Chatelier's flammability limit [27].

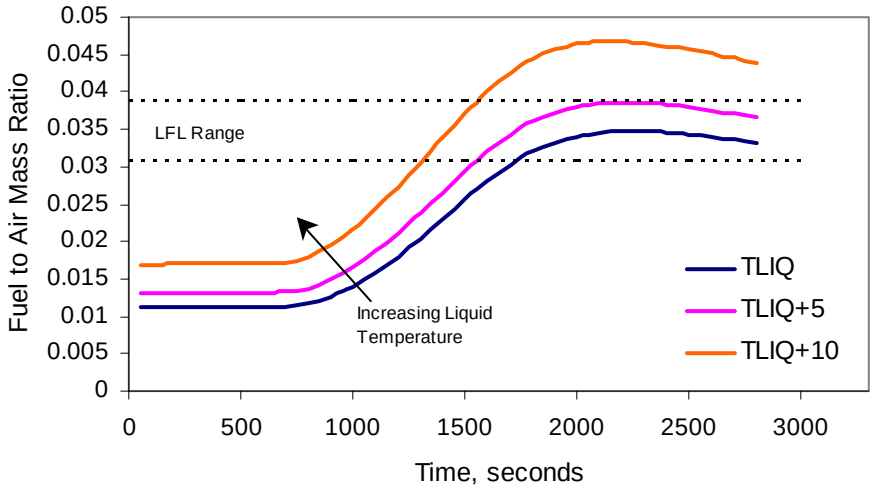

Figure 6.7. Liquid temperature effects on mixture flammability using the FAR rule [26]; heated tank at sea level with constant ambient temperature and pressure.

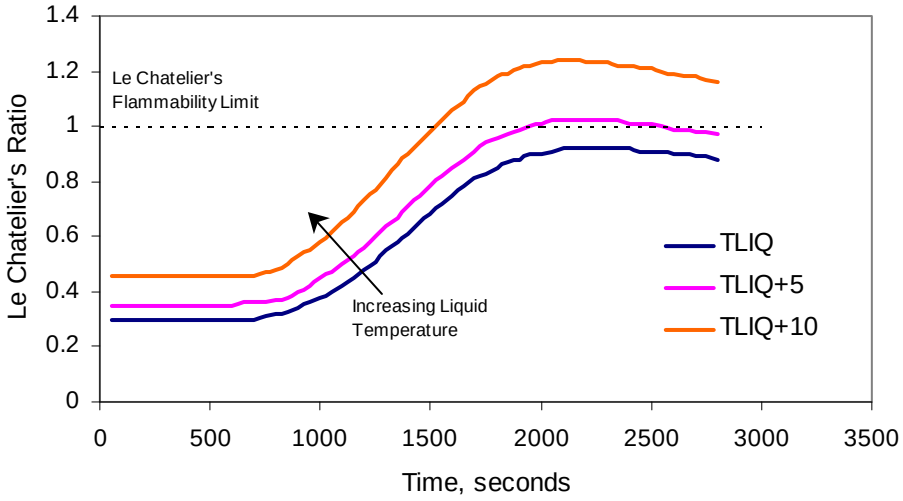

Figure 6.8. Liquid temperature effects on mixture flammability using Le Chatelier's flammability rule [27]; heated tank at sea level with constant ambient temperature and pressure.

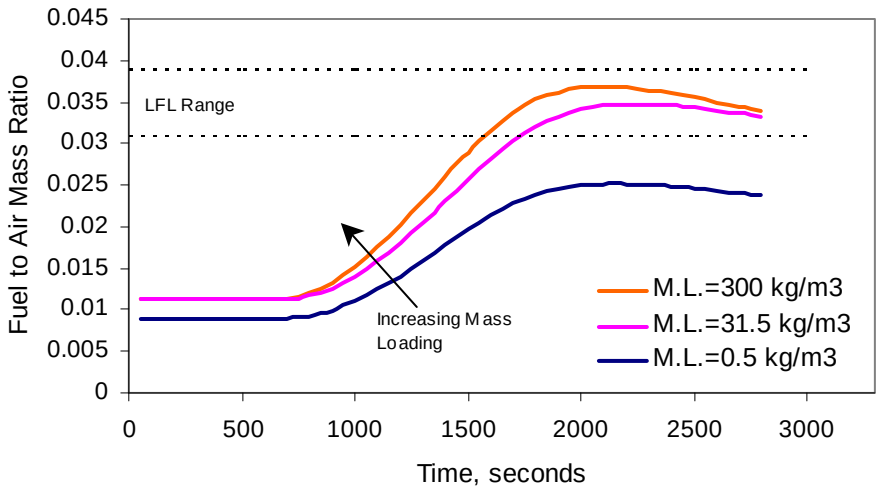

Figure 6.9. Mass loading effects on mixture flammability using the FAR rule [26]; heated tank at sea level with constant ambient temperature and pressure.

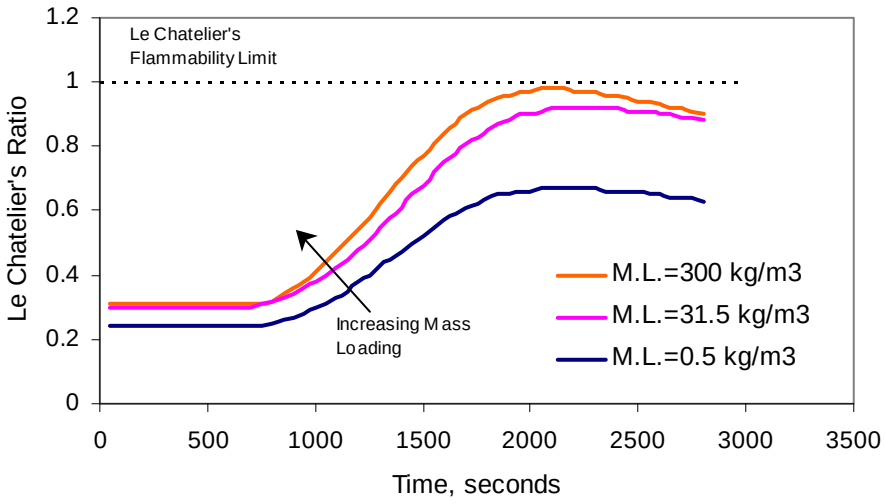

Figure 6.10. Mass loading effects on mixture flammability using Le Chatelier's flammability rule [27]; heated tank at sea level with constant ambient temperature and pressure.

6.2.2 Fuel Tank Under Varying Ambient Conditions

The FAR rule and Le Chatelier's ratio rule were again used to determine the level of flammability for the second example, an initially heated fuel tank exposed to simulated flight conditions. Figures 6.11 and 6.12 show, respectively, the calculated FAR and the calculated Le Chatelier's ratio, both calculated using the fuel compositions with flashpoints of 115°F and 120°F [21]. From figure 6.11, the mixture was not in the flammable region until the ambient pressure was decreased during ascent. This was due to the fact that the component vapor pressures are functions of temperature only, and although the ambient pressure outside of the fuel tank was decreasing, the component vapor pressures are fixed for the liquid fuel temperature. So in order for the fuel vapors to exert the same pressure on the enclosure at a reduced ambient pressure, more fuel molecules were required to vaporize into the ullage space. Le Chatelier's rule was again seen to be more conservative than the FAR rule by comparing figures 6.11 and 6.12, so the FAR rule will again be used to assess the effects of fuel temperature and mass loading on flammability for this flight profile test.

The liquid temperature effects on flammability are shown in figures 6.13 and 6.14. Three different liquid temperature profiles were used in the model to calculate the FAR and LCR using the fuel composition of the 115°F flashpoint fuel. The original average measured liquid temperature profile is referred to as TLIQ and the other two profiles were obtained by adding 5°F and 10°F to TLIQ and are referred to as TLIQ+5 and TLIQ+10, respectively. Figure 6.13 includes the predicted LFL range using the FAR criterion from reference [26]. It shows that for the conditions tested, the tank ullage was within the LFL range for part of the level flight at 30,000' altitude. However, increasing

the liquid fuel temperature by 5°F and 10°F resulted in significant broadening of the time period when the ullage was flammable to also include part of the ascent to 30,000'. Thus, the strong dependence of flammability on fuel temperature is again observed, as the period of flammability is broadened as liquid temperature is increased.

The effect of mass loading on flammability is shown in figures 6.15 and 6.16. Three different mass loadings were used in the model to calculate the FAR and LCR using the input data from the same flight profile test. The test was conducted with a mass loading of 31.5, while two other mass loadings, 300 kg/m^3 and 0.5 kg/m^3, were also used to calculate the respective FAR's and LCR to investigate the effect mass loading has on flammability. It can be seen that increasing the mass loading by about ten times barely increases the flammability, but decreasing the mass loading down to 0.5 kg/m^3 significantly decreases the flammability down to the borderline of the LFL range. Again, these results correlate well with the heated fuel tank at sea level and with previous experimental work [2].

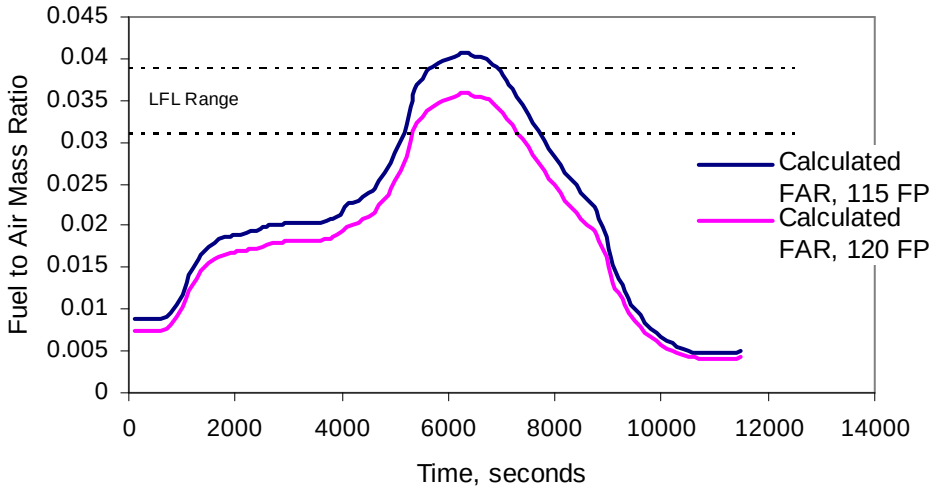

Figure 6.11. Temporal change in FAR for a flight profile test up to 30,000' altitude and range of the lower flammability limit [26].

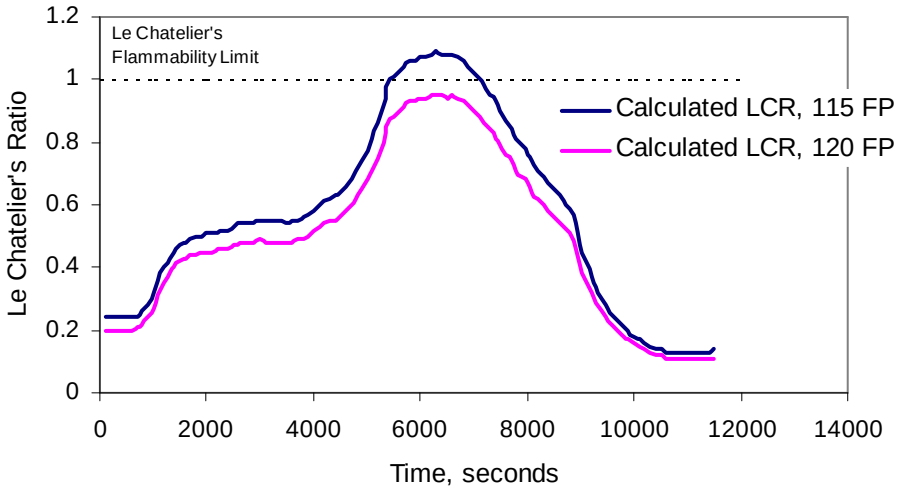

Figure 6.12. Calculated Le Chatelier's ratio for a flight profile test up to 30,000' altitude and Le Chatelier's flammability limit [27].

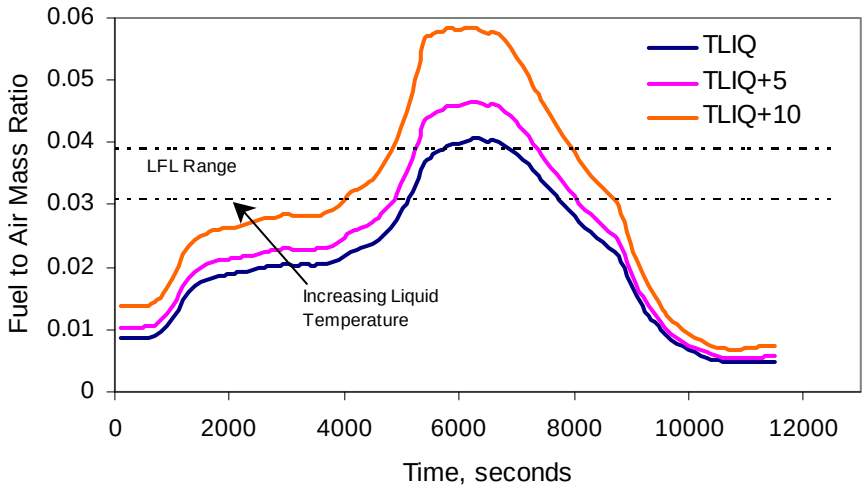

Figure 6.13. Liquid fuel temperature effects on flammability using the FAR rule [26]; flight profile test up to 30,000' altitude.

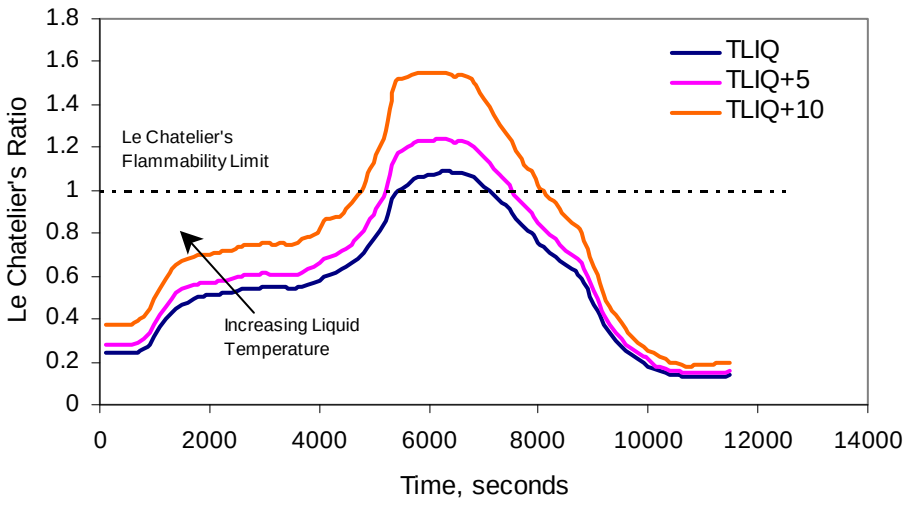

Figure 6.14. Liquid fuel temperature effects on flammability using Le Chatelier's flammability rule [27]; flight profile test up to 30,000' altitude.

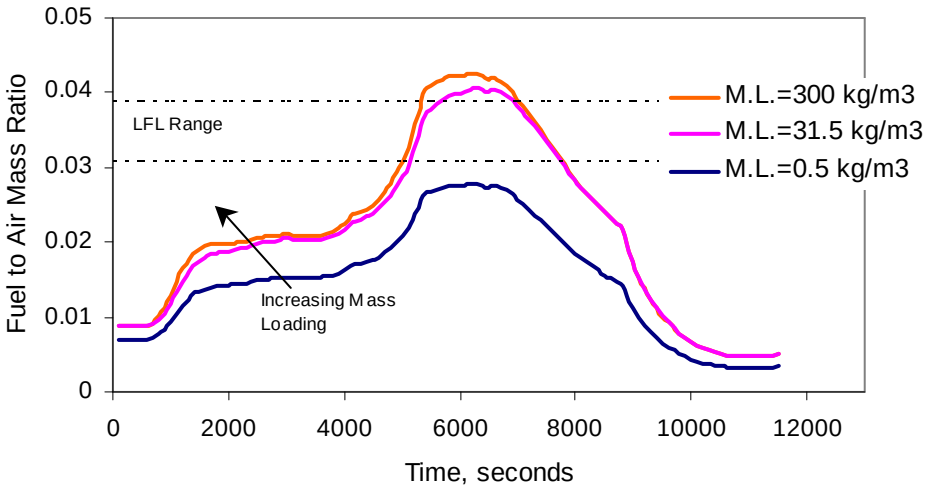

Figure 6.15. Mass loading effects on flammability using the FAR rule [26]; flight profile test up to 30,000' altitude.

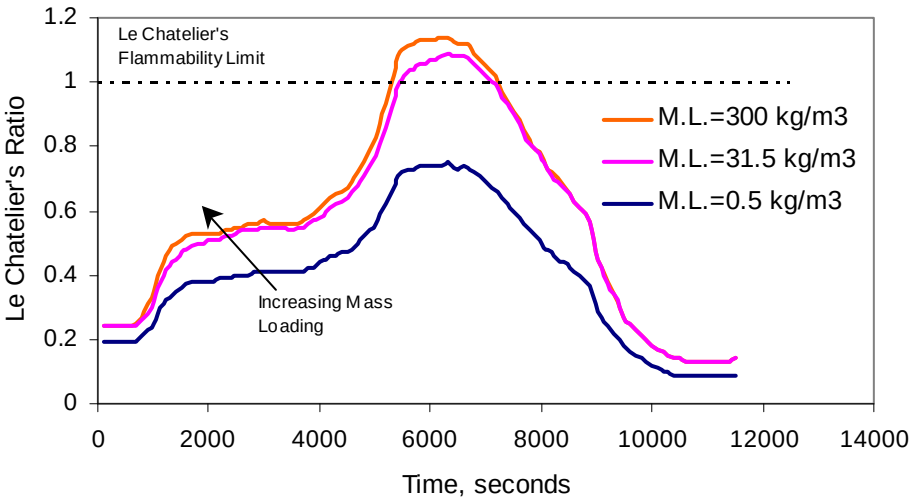

Figure 6.16. Mass loading effects on flammability using Le Chatelier's flammability rule [27]; flight profile test up to 30,000' altitude.

7.0 CONCLUSIONS AND RECOMMENDATIONS

The experimentation performed was successful in measuring ullage vapor concentration in a simulated aircraft fuel tank exposed to varying ambient conditions. A large set of data was collected that included fuel vaporization testing at constant ambient pressure and temperature, constant reduced ambient pressure, and flight profile tests with varying ambient conditions appropriate to in-flight aircraft fuel tank conditions. The data was useful in validating fuel vaporization model calculations from a pre-existing model. The model calculations of ullage gas temperature and vapor concentration proved to be in good agreement with experimentally measured data. The model was very useful in describing the transport processes occurring within the tank and evaluating the flammability in the experimental fuel tank. The flammability assessments indicated that Le Chatelier's rule was more conservative than the FAR rule, and that from a safety perspective the FAR rule should be used in differentiating between safe, non-flammable conditions and dangerously flammable conditions. The data generated has proven successful in validating a model and can be used for further validation work.

Further detailed experimental data on JP-8 flammability limits is required for further model validation, as well as laboratory testing in full sized aircraft fuel tanks and possibly testing from a fully instrumented fuel tank in an in-flight aircraft. Actual fuel tank testing would present several complications. Aircraft center wing tanks are divided into several different compartments that are connected via small openings in the partitions. This will complicate the internal flow field and possibly cause ullage gas stratification between the compartments. Also, it was seen in this work that the model calculations were heavily dependent upon the input temperatures; therefore accurate

temperature measurements would be required. In an in-flight aircraft, the liquid fuel is exposed to the forces of climbing, descending, and turbulence, causing fuel slosh and uneven liquid layer distribution. In order to measure a thin layer of fuel, it would require careful placement of the liquid thermocouples such that the thermocouple is fully immersed in the liquid at all times. Despite the complications presented by testing in an actual aircraft, the data generated would be extremely useful for further model validation and would provide a better understanding of the many processes occurring within an in-flight aircraft center wing tank.

APPENDIX A: REVIEW OF FUEL VAPORIZATION MODEL

The model used in this thesis is presented in reference [11] and will be summarized here in the appendix.

Several principal assumptions were made in the model to simplify the calculations. The flow field in the tank was assumed driven entirely by natural convection between the heated liquid fuel on the tank floor and the unheated tank ceiling and sidewalls. The ullage gas was considered well mixed with no thermal or concentration gradients existing within the ullage, which was justified by the fact that the natural convection flow in the tank was in the turbulent region, since the magnitude of the Raleigh number, based on the floor to ceiling temperature difference and the distance between them, was typically of order (10^9).

Initially it was assumed that the ullage gas mixture would be composed of *N* species, consisting of *N-1* fuel vapor components and atmospheric air. As the species concentrations were low for the purposes of these experiments, the vaporization rate of the fuel species considered was expressed by the relationship:

$$\dot{m}_{ei} = A_1 h_i \rho \left(y_{fi} - y_{gi} \right), i = 1 \to N \qquad (1)$$

The analogy between heat and mass transfer allowed for the species Sherwood number to be expressed in terms of the Nusselt number:

$$Sh_i = \frac{h_i L}{D_i} = Nu \left(\frac{Sc_i}{\Pr} \right)^{1/3} \qquad (2)$$

On the horizontal surfaces the Nusselt number was found by [38]:

$$Nu = 0.14 \left(Ra \right)^{1/3} \qquad (3)$$

Which is appropriate for Raleigh number of values larger than order (10^9), characterizing turbulent vertical mixing with the tank. The Nusselt number on the vertical enclosure surfaces was expressed using laminar free-convection from a vertical surface [35]:

$$Nu = 0.664(\mathrm{Re})^{1/2}(\mathrm{Pr})^{1/3} \quad (4)$$

Where the Reynolds number was based on the free convection velocity and the height of the tank. The liquid surface species mole fraction was computed using Henry's Law:

$$x_{fi} = \frac{x_{1i}\, p_i}{p}, i = 1 \rightarrow N-1 \quad (5)$$

The gas species mass fractions were related to the species mole fractions by the relationship:

$$y_i = \frac{x_i M_i}{\sum_{i=1}^{N} x_i M_i}, i = 1 \rightarrow N \quad (6)$$

The liquid density was given by:

$$\rho_l = \frac{\sum_{i=1}^{N-1} x_{li} M_i}{\sum_{i=1}^{N-1} \frac{x_{li} M_i}{\overline{\rho}_{li}}} \quad (7)$$

The thickness of the liquid fuel layer was computed using the liquid density, the sum of the vaporization rate of all species, and the liquid surface area.

In addition to vaporization of the fuel on the test tank floor, there was condensation of vapor species occurring on the tank ceiling and the tank walls beginning when the wall temperature was equal to or below the dew point temperature of the ullage gas mixture. The previous equations were used to estimate the condensation rate on the tank ceiling and sidewalls. Condensation was assumed to produce a thin static liquid film

layer of spatially uniform but temporally varying temperature and thickness, with the condensate layer temperature equal to the tank wall temperature.

The species mass balance for the control volume defined by the bulk gas within the ullage, including the rate of species vaporization, condensation, and outflow:

$$\dot{m}_i = (\dot{m}_{ei} - \dot{m}_{ci})(1 - \delta_{iN}) \pm \dot{m}_{oi}, i = 1 \to N \qquad (8)$$

Gases were assumed to follow ideal gas behavior so that m_i was written as:

$$m_i = \frac{x_i M_i pV}{\bar{R} T_g}, i = 1 \to N \qquad (9)$$

Substituting and solving for the variation of species mole fraction within the gas control volume:

$$\dot{x}_i = \frac{\bar{R} T_g}{M_i V p}\left[(\dot{m}_{ci} - \dot{m}_{ei})(1 - \delta_{iN}) \pm \dot{m}_{oi} - \frac{m_i}{p}\frac{dp}{dt} + \frac{m_i}{T_g}\frac{dT_g}{dt} \right], i = 1 \to N \qquad (10)$$

Summation of the terms in equation 10 over all species resulted in the following relationship for the total rate of mass inflow or outflow:

inflow: $-\dot{m}_o \sum_{i=1}^{N} \frac{1}{M_i} =$

$$\sum_{i=1}^{N} \frac{1}{M_i}(\dot{m}_{ci} - \dot{m}_{ei})(1 - \delta_i) - \sum_{i=1}^{N} \frac{m_i}{M_i p}\frac{dp}{dt} + \sum_{i=1}^{N} \frac{m_i}{M_i T_g}\frac{dT_g}{dt}, i = 1 \to N \qquad (11)$$

outflow: $\frac{\dot{m}_o}{M} =$

The ullage control volume energy balance was given by the following relationship, which was used to compute the ullage temperature:

$$\frac{d}{dt}\left(m_g c_{pg} T_g\right) = \bar{h}_b A_b \left(T_b - T_g\right) - \bar{h}_t A_t \left(T_g - T_s\right) - \bar{h}_s A_s \left(T_g - T_s\right) + \dot{m}_c H_v + \dot{m}_e c_{pv} T_l - \dot{m}_c c_{pg} T_g$$

For inflow: $+\dot{m}_o c_{pa} T_a$

(12)

For outflow: $-\dot{m}_o c_{pg} T_g$

The left hand side of equation 12 was the rate of energy storage, the first three terms on the right side were the rates of heat transfer from the floor, the ceiling, and the sidewalls, respectively, the fourth term on the right was the latent heat release during condensation, and the last three terms on the right side were the rates of energy transfer associated with the evaporating, condensing, and vent gas fluid streams, respectively.

Species vapor pressures were estimated using Wagner's or Frost-Kalkwarf-Thodos's equations [28]. The species diffusion coefficients were estimated using Fuller's method [28], and for the low vapor concentrations considered, the gas viscosity and thermal conductivity used with the non-dimensional parameters in equations 2, 3, and 8 were taken from data for pure air at the corresponding liquid-gas film temperature [35]. The ullage gas specific heat, c_{pg}, was also that of pure air at the ullage gas temperature. The mean specific heat of the evolving vapors was computed at the liquid-ullage gas film temperature using the correlation of reference (36) and the mean condensate latent heat of condensation was 3.6×10^5 J/kg, approximately equal to that of Jet A at 30°C from reference (37).

APPENDIX B: ABBREVIATIONS AND TERMINOLOGY

APU: Auxiliary Power Unit

CWT: Center Wing Tank

DAS: Data Acquisition System

ECS: Environmental Control System

FAA: Federal Aviation Administration

FAR: Fuel to Air mass Ratio

FID: Flame Ionization Detector

LCR: Le Chatelier's Ratio

LFL: Lower Flammability Limit

LOC: Lower Oxygen Concentration

NEA: Nitrogen Enriched Air

NTSB: National Transportation Safety Board

OBIGGS: On Board Inert Gas Generation System

PPM: Parts Per Million propane equivalent; quantifies volumetric concentration of fuel

THC: Total Hydrocarbon Concentration

Ullage: The space in the fuel tank unoccupied by liquid fuel; vapor space

APPENDIX C: EXPERIMENTAL FUEL FLASHPOINT TEST RESULTS

TROTEST INSTRUMENTS BERLIN TEL. 030-7219036 TAG2

NO	TEST NO	PROG	E-FLP (°C)	FLP (°C)	MIN.	DATE	
	Sample						FLP °C
???? #1	03	TAG	050	048.0	11	04:14:04	46.8
???? #2	04	TAG	050	048.1	11	04:14:04	46.8

REFERENCES

1. National Transportation Safety Board, In-Flight Breakup Over the Atlantic Ocean Trans World Airlines Flight 800 Boeing 747-131 N93119 Near East Moriches, NY July 17, 1996, NTSB/AAR-00/03.

2. Summer, S.M., Mass Loading Effects on Fuel Vapor Concentrations in an Aircraft Fuel Tank Ullage, FAA Report #DOT/FAA/AR-TN99/65, September 1999

3. Nestor, L.J., Investigation of Turbine Fuel Flammability Within Aircraft Fuel Tanks. FAA Report #FAA-DS-67-7. July 1967.

4. Zabetakis et al. Research on the Flammability Characteristics of Aircraft Fuels. WADC Technical Report 52-35 United States Dept. of the Interior. 1952.

5. Zinn, S.V. Inerted Fuel Tank Oxygen Concentration Requirements. FAA Report #FAA-RD-71-42, August 1971.

6. Kosvic, T.C., Laurence, B.Z., and Gerstein, M., Analysis of Aircraft Fuel Tank Fire and Explosion Hazards, 1971, AFAPL-TR-71-7.

7. Summer, S.M., Cold Ambient Temperature Effects on Heated Fuel Tank Vapor Concentrations, FAA Report #DOT/FAA/AR-TN99/93, July 2000.

8. Burns, M. et al., Evaluation of Fuel Tank Flammability and the FAA Inerting System on the NASA 747 SCA," DOT/FAA/AR-04/41, December 2004.

9. Summer, S.M., Limiting Oxygen Concentration Required to Inert Jet Fuel Vapors Existing at Reduced Fuel Tank Pressures – Final Phase, DOT/FAA/AR-04/8, August 2004.

10. Shepherd, J.E., Krok, C, and Lee, J.J., Spark Ignition Energy Measurements in Jet A. Explosion Dynamics Laboratory Report FM97-9. 1997.

11. Polymeropoulos, C.E. and Ochs, R. "Jet A Vaporization in a Simulated Aircraft Fuel Tank (Including Sub-Atmospheric Pressures and Low Temperatures)," Presented at the Fourth International Aircraft Fire and Cabin Research Conference, Lisbon, Portugal, November 15-18, 2004.

12. Summer, S.M., Flammability Characteristics of JP-8 Fuel Vapors Existing within a Typical Aircraft Fuel Tank, Masters Degree Thesis submitted to the Graduate School-New Brunswick, Rutgers, the State University of New Jersey, January 2001.

13. Fuel Flammability Task Group, A Review of the Flammability Hazard of Jet A Fuel Vapor in Civil Transport Aircraft Fuel Tanks, Final Report, FAA Report #DOT/FAA/AR-98/26, June 1998.

14. Chevron Products Company. Aviation Fuels Technical Review (FTR-3). A division of Chevron USA. 2000.

15. Clodfelter, R.G. Fire Safety in Military Aircraft Fuel Systems. *Proceedings from the Committee on Aviation Fuels with Improved Fire Safety*.

16. ASTM D 1655-97. Specification for Aviation Turbine Fuels, in *1998 Book of Standards, Vol. 05.01*, ASTM, West Conshohocken, PA, 1998.

17. Shepherd, J.E., Nuyt, C.D., and Lee, J.J., Flash Point and Chemical Composition of Aviation Kerosene (Jet A), Explosion Dynamics Laboratory Report FM99-4. 1999.

18. Nave, C.R. HyperPhysics. Department of Physics and Astronomy, Georgia State University. 2000.

19. Atkins, P. and Jones, L. Chemistry: Molecules, Matter, and Change, W.H.Freeman and Company, New York, 1997, 3rd edition.

20. Naegeli, D.W. and Childress, K.H., Lower Explosion Limits and Compositions of Jet Fuel Vapors, presented at the Western States Section/Combustion Institute, at the University of California, Berkeley, 1998.

21. Woodrow, J. E., The Laboratory Characterization of Jet Fuel Vapor and Liquid, *Energy and Fuels, 2003,17:216-224.*

22. Glassman, I. Combustion, Academic Press, New York, 1996, 3rd edition.

23. Bunama, R., Karim, G.A., and Zhang, C.Y., An Investigation of the Formation and Venting of Flammable Mixtures Formed Within Liquid Fuel Vessels, *Journal of Engineering for Gas Turbines and Power, 1999, 121:68-73.*

24. Huber, M.L. and Yang, J.C., A Thermodynamic Analysis of Fuel Vapor Characteristics in an Aircraft Fuel Tank Ullage, *Fire Safety Journal, 2002, 37:517-524.*

25. Figliola, R.S., Beasley, D.E. Theory and Design for Mechanical Measurements. John Wiley & Sons, Inc. New York. 2000. 3rd ed.

26. Kuchta, J.M., Investigation of Fire and Explosion Accidents in the Chemical, Mining, and Fuel Related Industries, U.S. Department of the Interior, Bureau of Mines Bulletin 680, 1985.

27. Affens, W.A. and McLaren, G.W., Flammability Properties of Hydrocarbon Solutions in Air, J. Chemical and Engineering Data, 1972, 17:482:488.

28. Polling, B.E., Prausnitz, J.M., and O'Connell, J.P., The Properties of Gases and Liquids, McGraw-Hill, New York, 2000.

29. Shepherd, J.E., Krok, J.C., and Lee, J.J., Jet A Explosion Experiments: Laboratory Testing, 1997, Docket SA-516, Exhibit 20D, National Transportation Safety Board.

30. Catton, I., Natural Convection in Enclosures, 6th Int. Heat Transfer Conf., 1978, 6:13-31, Toronto.

31. Hoogendoon, C.J., Natural Convection in Enclosures, 8th Int. Heat Transfer Conf., 1986, 1:111-120, San Francisco.

32. Ostrach, S., Natural Convection in Enclosures, J. Heat Transfer, 1988, 110:1175-1190.

33. Roth, A.J., Development and Evaluation of an Airplane Fuel Tank Ullage Composition Model, v.II-Experimental Determination of Airplane Fuel Tank Ullage Compositions, Boeing, AFWAL-TR-2060, 1987.

34. Birk, A.M., A Study of Fire Heating of a Propane Tank Located Near a Burning Building, J. Applied Fire Science, 2000, 9:173-1999.

35. Incropera, F.P., and DeWitt, D.P., Fundamentals of Heat and Mass Transfer, 4th ed., Wiley, New York, 1996.

36. Lefebvre, A., Gas Turbine Combustion, Hemisphere, Washington, 1983.

37. Handbook of Aviation Fuel Properties, 1988, CRC Rpt. 530, Society of Automotive Engineers, Warrendale.

38. Hollands, K.G.T., Raithby, G.D., and Konicek, L., Correlation Equations for Free Convection Heat Transfer in Horizontal Layers of Air and Water, Int. J. Heat Mass Transfer, 1975, 18:879-884.